nature metabolism

Article

https://doi.org/10.1038/s42255-026-01619-4

Metabolic and neural responses to ultraprocessed foods: a randomized, controlled, crossover study

Received: 13 April 2026

Accepted: 21 August 2026

Published online: 05 October 2026

Check for updates

Zach Hutelin[1,2], Monica Ahrens[3,4,5], Mary Elizabeth Baugh[2], Emmanuel Nartey[3,5], Delbert L. Herald III[2], Alexandra L. Hanlon[3,5] & Alexandra G. DiFeliceantonio[2,6]

Dietary patterns worldwide have shifted toward increased consumption of ultraprocessed foods (UPFs), which has been linked to higher disease burden. One proposed mechanism underlying both UPF consumption and metabolic disease is altered post-ingestive responses relative to nutritionally similar foods. Here we report the effects of food processing on post-ingestive metabolism and brain response in a randomized, crossover study involving 57 healthy-weight adults who consumed a nutritionally matched UPF or non-UPF meal. We show that despite being nutritionally similar, UPF meals evoke greater insulinaemic and energetic responses, with attenuated carbohydrate oxidation relative to non-UPF meals. Between-condition differences in peak carbohydrate oxidation are associated with striatal activation in response to food cues. We also find that although subjective food value does not differ between conditions, brain responses correlated with food valuation are positive for non-UPF but negative for UPF in the visual cortex and striatum. Overall, these findings suggest that food processing influences post-ingestive metabolic and neural responses through mechanisms beyond calories and macronutrients alone.

The modern food environment has undergone a shift towards widespread availability of UPFs[1,2]. Under the Nova classification system, UPFs are industrially manufactured products that undergo multiple physical and chemical transformations and typically contain added industrial ingredients, specifically additives not commonly used in home cooking[3]. Concerningly, higher UPF intake is associated with poorer health outcomes, including cancer, overweight and obesity, and metabolic dysfunction[4,5]. Despite these adverse health associations, UPFs comprise the majority of calories consumed in the United States and most of the food market[1,2]. Although the mechanistic basis for UPF-associated health effects is not fully established, the incorporation of manufacturing processes that alter nutritional availability has been proposed as a potential factor[5].

Even with the same ingredients, micronutrient bioavailability differs after food processing[6]. For macronutrients, industrial extrusion divides starches to produce a spectrum of fractions, granules and crystalline structures, augmenting digestibility and resulting in distinct glycaemic and insulinaemic properties[7]. For example, compared with steel-cut, instant oats that have been cooked at higher temperatures to partially gelatinize the starch elicit a higher glycaemic index despite still only containing oats[8]. Varying the cellular microstructure of chickpeas, including disrupting cell walls as seen in many UPFs,

[1]Translational Biology, Medicine, and Health Graduate Program, Virginia Tech, Roanoke, VA, USA. [2]Fralin Biomedical Research Institute at VTC, Virginia Tech, Roanoke, VA, USA. [3]Center for Biostatistics and Health Data Science, Virginia Tech, Roanoke, VA, USA. [4]Division of Medical Informatics, University of Kansas Medical Center, Kansas City, KS, USA. [5]Department of Statistics, Virginia Tech, Blacksburg, VA, USA. [6]Department of Human Nutrition, Foods, and Exercise, Virginia Tech, Blacksburg, VA, USA. e-mail: dife@vt.edu

produced larger postprandial glucose and insulin excursions and greater concentrations of glucose and maltose in the duodenum[9]. Although evidence that food processing could lead to altered metabolic function is accumulating, much of it comes from studies that did not explicitly test foods that differ on the Nova score while controlling for nutritional composition.

If UPFs elicit augmented physiological responses owing to altered nutritional availability relative to nutritionally matched foods that are not ultraprocessed, not only could this provide a potential mechanism for their effects on metabolic health but also may represent a key mechanism contributing to their overconsumption. Foods high in both fat and sugar, as seen in many UPFs, are valued more than foods high in fat or sugar alone and elicit responses in regions critical for reward valuation, such as the striatum[10,11]. Moreover, this difference in food value is thought to be learned in part through gut-to-brain signalling driven by post-ingestive metabolic responses, known as flavour-nutrient learning[12–14]. The magnitude of the post-ingestive metabolic response to sugar-sweetened beverages has been associated with changes in rated liking and food-cue reactivity in the striatum, evidence for flavour-nutrient learning in humans[15,16]. This nutrient information is thought to be relayed from the duodenum, where nutrients cross the brush-border membrane, to the brain[17–19]. Collectively, these findings support a framework in which UPFs may amplify gut-to-brain signalling by increasing nutrient exposure at the proximal small intestine, the site of greatest nutrient absorption[19], and leading to changed food valuation and consumption[12,13,20].

To test this hypothesis, we characterized the post-ingestive response to nutrient-matched meals that differed in level of processing according to the Nova classification system. Next, we tested whether these processing-related differences in post-ingestive metabolism are associated with neural responses to food pictures and subjective food value. These findings identify potential post-ingestive mechanisms for overconsumption of foods, including UPFs, that extend beyond caloric and macronutrient composition alone.

Results

Participant characteristics

The full study comprised 57 participants; of these, 32 completed both metabolic sessions in a randomized crossover design and 52 completed the functional magnetic resonance imaging (fMRI) session (Extended Data Fig. 1). Every participant who completed the metabolic sessions also completed the fMRI session. The overall participant sample was 31.6% male, with a mean age of 26.21 ± 6.85 years and body mass index (BMI) of 22.75 ± 1.87 kg m^{-2} (Extended Data Table 1). Participants' habitual energy intake on average comprised 54.4 ± 18.4% UPFs, similar to the national average of 55.0% (ref. 2). Additional participant characteristics are described in Extended Data Table 1. Exclusions and final analytic samples for each modality are summarized in the CONSORT diagram (Extended Data Fig. 1).

Acute metabolic effects of UPFs and non-UPFs

To investigate the effect of processing level on post-ingestive metabolic response to foods with matched nutrient content, 32 participants consumed, and were required to finish within 10 min, ~300 kcal nutritionally matched meals composed entirely of either UPF or non-UPF while undergoing 4 h (50 min baseline followed by a 3 h postprandial period) of whole-room indirect calorimetry (WRIC) and concomitant blood collection by intravenous catheter (Fig. 1a). The non-UPF and UPF test meals were closely matched on meal weight, energy, energy density, macronutrients, available carbohydrate, glycaemic index and load, total dietary fibre, sodium and water (all ≤1.6% deviation between meals; Fig. 1b). The meals were consumed on separate days in a randomized crossover design, allowing within-participant comparison of indirect calorimetry and blood-derived metabolic outcomes (see Methods for session timing).

Data collection was performed in the morning, and participants were instructed to fast overnight. Time since last meal was recorded before data collection. Self-reported time since last meal did not differ between the non-UPF and UPF conditions ($t(30.46) = -1.31$; $P = 0.20$; 95% CI, −0.21 to 0.96). Total energy intake on the day preceding the metabolic session did not differ between conditions ($t(30.90) = 1.30$; $P = 0.20$, 95% CI, −440.2 to 97.55); macronutrient intake also did not differ between conditions (carbohydrate, $P = 0.07$; fat, $P = 0.58$; protein, $P = 0.37$).

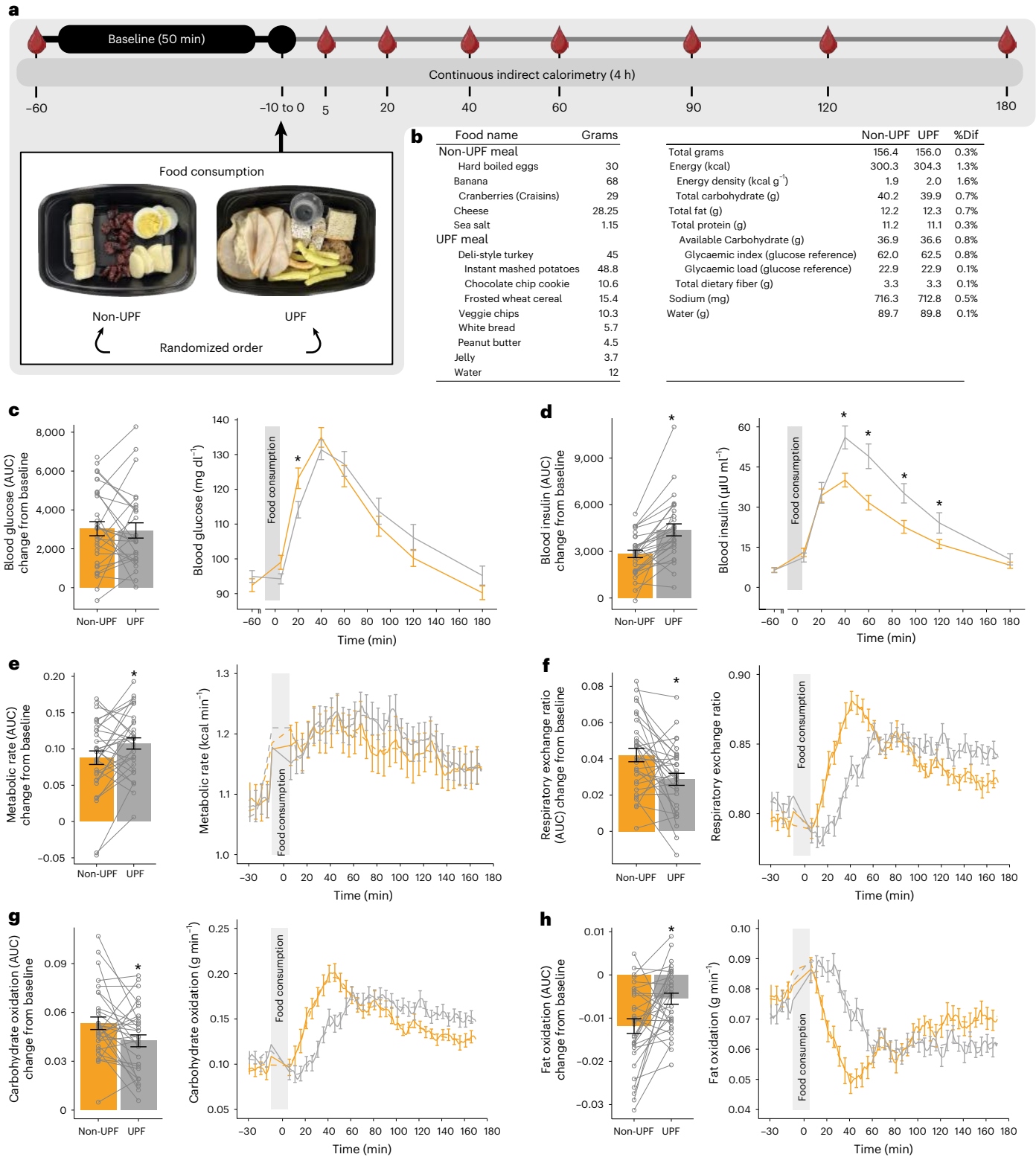
During the 50 min baseline resting metabolic measures, wrist and ankle accelerometry indicated low movement and no statistically significant differences in movement between conditions ($t(28.46) = 1.73$; $P = 0.10$; 95% CI, −1771.61 to 150.57; Extended Data Fig. 2a). Baseline blood glucose ($t(26.46) = 1.43$; $P = 0.17$; 95% CI, −5.11 to 0.93) and insulin ($t(28.91) = 0.04$; $P = 0.97$; 95% CI, −2.27 to 2.09) did not differ between conditions (Extended Data Fig. 2b,c). WRIC baseline measures were calculated by averaging the 15 min before test-meal consumption (minutes −30 to −15). Baseline metabolic rate ($t(30.10) = 0.06$; $P = 0.95$; 95% CI, −0.02 to 0.02), respiratory exchange ratio (RER) ($t(29.99) = 1.41$; $P = 0.17$; 95% CI, −0.024 to 0.004), carbohydrate oxidation ($t(30.49) = 1.40$; $P = 0.17$; 95% CI, −0.023 to 0.004) and fat oxidation ($t(29.95) = -1.22$; $P = 0.23$; 95% CI, −0.003 to 0.01) did not differ between conditions (Extended Data Fig. 2d–g).

After the 50 min baseline measures, participants were instructed to consume all of the test meal in under 10 min. Ratings of the participants' internal state (hunger, fullness and thirst) were collected at the start of the baseline measurement, immediately after meal consumption, 60 min post meal and at the end of the metabolic measurement (180 min). The UPF meal was consumed more slowly than the non-UPF meal by an average of 1.5 min ($t(30.43) = 5.13$; $P < 0.001$; 95% CI, −1.82 to −0.78; Extended Data Fig. 3a). Immediately after meal consumption, participants rated meal liking ($t(30.13) = 0.61$; $P = 0.55$; 95% CI, −15.07 to 8.12) and wanting ($t(30.87) = 0.73$; $P = 0.47$; 95% CI, −12.41 to 5.88), which were not statistically different between conditions (Extended Data Fig. 3b,c). There were no time-by-condition interactions for rated hunger ($\chi^2(3) = 2.05$; $P = 0.56$), fullness ($\chi^2(3) = 6.19$; $P = 0.10$) or thirst ($\chi^2(3) = 0.76$; $P = 0.86$; Extended Data Fig. 3d–f).

Blood samples were obtained intravenously at minutes −60 (baseline), 5, 20, 40, 60, 90, 120 and 180 after consuming the test meal (Fig. 1a). Consistent with the meals being matched on glycaemic index, blood glucose area under the curve (AUC) did not differ significantly between conditions ($t(27.15) = -0.11$; $P = 0.92$; 95% CI, −738.2 to 813.21; Fig. 1c). However, when we examined blood glucose trajectories over time, we observed a significant time-by-condition interaction ($\chi^2(7) = 23.60$; $P = 0.001$). Specifically, blood glucose rose more rapidly in the non-UPF condition, with higher concentrations at 20 min post meal ($t(426.30) = -3.10$; $P = 0.02$; 95% CI, −17.58 to −1.05, corrected; Fig. 1c), and both conditions peaked at 40 min. However, glucose remained elevated later in the UPF condition, trending higher at 120 and 180 min and failing to return to baseline in the same manner as the non-UPF condition. Despite comparable blood glucose AUC, blood insulin AUC differed significantly between conditions, with the UPF condition evoking a markedly greater insulin response ($t(28.67) = 5.48$; $P < 0.001$; 95% CI, −2254.02 to −1032.03; Fig. 1d). Insulin also showed a significant time-by-condition interaction ($\chi^2(7) = 45.43$; $P < 0.001$). Concentrations were similar at 5min and 20 min; however, insulin was greater in the UPF condition at minutes 40, 60, 90 and 120 (all $P < 0.05$), with both conditions returning to near-baseline values at 180 min (Fig. 1d). Together, these findings indicate that although peak blood glucose concentrations were similar between meals, the UPF condition evoked a greater insulinaemic response.

We next evaluated 3 h postprandial metabolic responses collected using WRIC. Despite both conditions having the same caloric load, post-ingestive metabolic rate AUC was greater after the UPF meal ($t(30.73) = 2.39$; $P = 0.02$; 95% CI, −0.036 to −0.003; Fig. 1e). Metabolic

https://doi.org/10.1038/s42255-026-01619-4



Food name	Grams
Non-UPF meal	
Hard boiled eggs	30
Banana	68
Cranberries (Craisins)	29
Cheese	28.25
Sea salt	1.15
UPF meal	
Deli-style turkey	45
Instant mashed potatoes	48.8
Chocolate chip cookie	10.6
Frosted wheat cereal	15.4
Veggie chips	10.3
White bread	5.7
Peanut butter	4.5
Jelly	3.7
Water	12

	Non-UPF	UPF	%Dif
Total grams	156.4	156.0	0.3%
Energy (kcal)	300.3	304.3	1.3%
Energy density (kcal g^{-1})	1.9	2.0	1.6%
Total carbohydrate (g)	40.2	39.9	0.7%
Total fat (g)	12.2	12.3	0.7%
Total protein (g)	11.2	11.1	0.3%
Available Carbohydrate (g)	36.9	36.6	0.8%
Glycaemic index (glucose reference)	62.0	62.5	0.8%
Glycaemic load (glucose reference)	22.9	22.9	0.1%
Total dietary fiber (g)	3.3	3.3	0.1%
Sodium (mg)	716.3	712.8	0.5%
Water (g)	89.7	89.8	0.1%

Fig. 1 | Nutritionally matched ultraprocessed and non-ultraprocessed meals elicit different postprandial responses. a, Session flow and timing of blood draws with a picture of each meal as it was given to participants. **b**, Meals were composed of different food sources and were nutritionally matched. **c**, Blood glucose AUC did not differ between conditions ($t(27.15) = -0.11$; $P = 0.92$; 95% CI, −738.2 to 813.21); however, there was a significant time-by-diet interaction, such that non-UPF blood glucose level was higher than UPF at minute 20 ($\chi^2(7) = 23.60$; $P = 0.001$). **d**, Blood insulin AUC was greater in the UPF condition ($t(28.67) = 5.48$; $P < 0.001$; 95% CI, −2254.02 to −1032.03), and a significant time-by-diet interaction was observed such that insulin levels were higher between 40 and 120 min after consumption of the UPF compared with non-UPF meals ($\chi^2(7) = 45.43$; $P < 0.001$). **e**, Metabolic rate AUC was greater in the UPF condition ($t(30.73) = 2.39$; $P = 0.02$; 95% CI, −0.036 to −0.003). **f**, RER AUC was greater in the non-UPF condition ($t(30.75) = -3.04$; $P = 0.01$; 95% CI, 0.004–0.022). **g**,**h**, This difference is reflected in lower carbohydrate oxidation AUC after consumption of non-UPF compared with UPF meals ($t(30.76) = -2.47$; $P = 0.02$; 95% CI, 0.002–0.019) (**g**) and greater fat oxidation AUC in the UPF condition ($t(30.84) = 3.26$; $P = 0.003$; 95% CI, −0.01 to −0.002) (**h**). Each dot represents a participant; error bars, s.e.m. $n = 32$ participants for all analyses except blood insulin ($n = 31$ participants). *$P < 0.05$; all tests are two-tailed. Created in BioRender; Hutelin, Z. https://biorender.com/8mxvats (2026).

https://doi.org/10.1038/s42255-026-01619-4

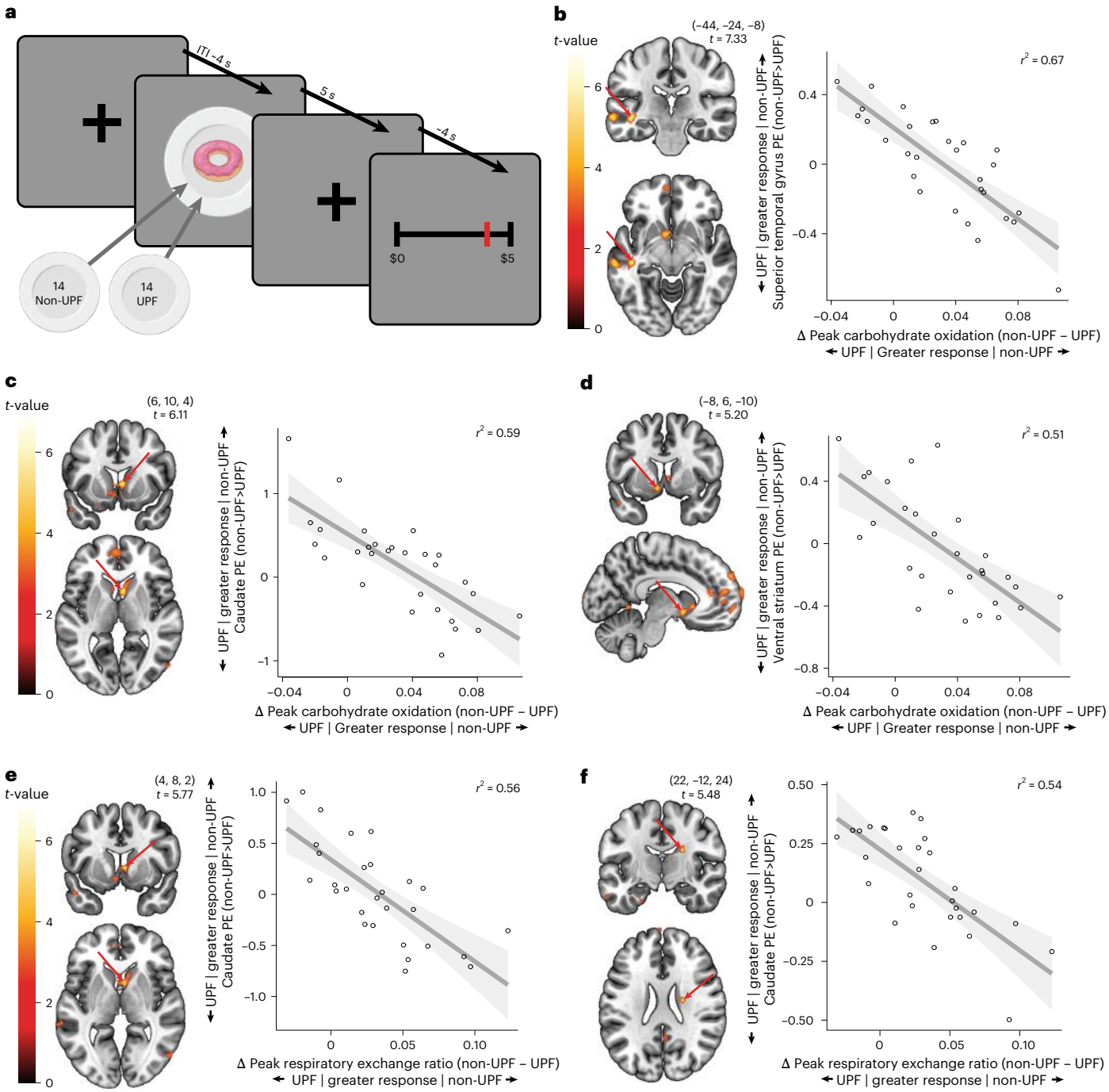


Fig. 2 | Differences in metabolic response between ultraprocessed and non-ultraprocessed meals are associated with differences in neural response to food cues. a, Participants saw 14 non-UPF and 14 UPF items in a random order with a jittered intertrial interval (ITI) before rating their willingness to pay for that item. **b**, A higher response in the superior temporal gyrus to non-UPF pictures relative to UPF was associated with less carbohydrate oxidation to UPF ((−44, −24, −8); $t = 7.33$; $P_{FWE} = 0.013$). **c**,**d**, After SVC of an a priori striatal region of interest (ROI), associations in the same direction were also observed in caudate ((6, 10, 4); $t = 6.11$; SVC $P_{FWE} = 0.007$) (**c**) and ventral striatum ((−8, 6, −10); $t = 5.20$; SVC $P_{FWE} = 0.045$) (**d**) for carbohydrate oxidation, and in **e**,**f**, caudate for respiratory exchange ratio ((4, 8, 2); $t = 5.77$; SVC $P_{FWE} = 0.014$; (**e**) (22, −12, 24); $t = 5.48$; SVC $P_{FWE} = 0.026$ (**f**)). Arrows point to the significant FWE-corrected peak displayed within a cluster threshold of $P_{uncorrected} < 0.001$. $n = 29$ participants. All r^2, $P < 0.0001$; error bands, 95% CI. PE, parameter estimate. Created in BioRender; Hutelin, Z. https://biorender.com/msvyhzj (2026).

rate increased similarly in both conditions and peaked at ~40 min; however, after this peak, metabolic rate declined more in the non-UPF condition than in the UPF condition. By contrast, RER AUC was higher after the non-UPF meal ($t(30.75) = -3.04$; $P = 0.01$; 95% CI, 0.004–0.022; Fig. 1f). Notably, the meals were matched with respect to macronutrient composition, yet the RER response indicates differential substrate partitioning. Consistent with this observation, carbohydrate oxidation followed the same pattern as RER, with a greater response at minute 40 following the non-UPF meal compared to the UPF meal ($t(30.76) = -2.47$; $P = 0.02$; 95% CI, 0.002–0.019; Fig. 1g), whereas fat oxidation demonstrated the reciprocal pattern ($t(30.84) = 3.26$; $P = 0.003$; 95% CI, −0.01 to −0.002; Fig. 1h). To explore the effects of habitual dietary intake on

https://doi.org/10.1038/s42255-026-01619-4

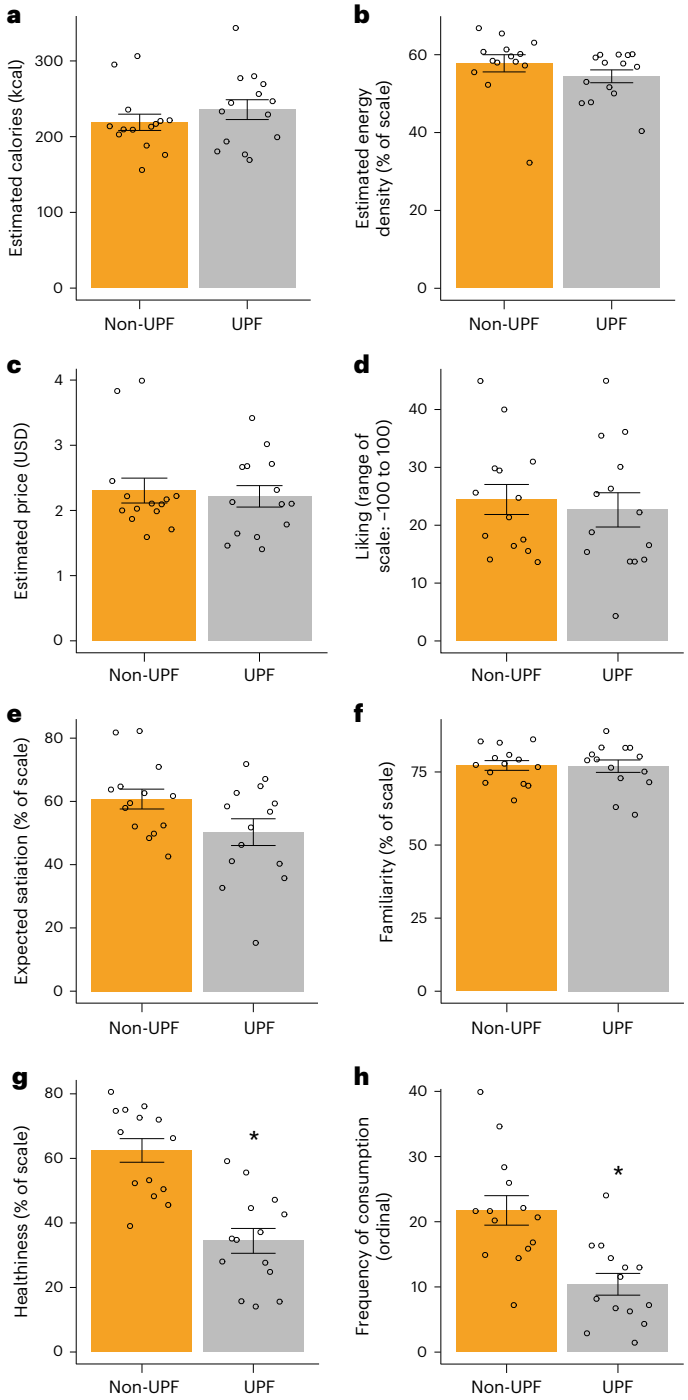


Fig. 3 | Participant ratings of food stimuli. a–**f**, Participants rated estimated calories ($t(26) = 0.99$; $P = 0.33$; 95% CI, −51.55 to 18.08) (**a**), estimated energy density ($t(26) = -1.21$; $P = 0.24$; 95% CI, −23.28 to 90.03) (**b**), estimated price ($t(26) = -0.35$; $P = 0.73$; 95% CI, −0.43 to 0.61) (**c**), liking ($t(26) = -0.46$; $P = 0.65$; 95% CI, −6.29 to 9.89) (**d**), expected satiety ($t(26) = -1.99$; $P = 0.06$; 95% CI, −0.37 to 21.28) (**e**) and familiarity ($t(26) = -0.09$; $P = 0.93$; 95% CI, −5.31 to 5.79) (**f**) similarly between conditions. **g**,**h**, In this sample, participants' ratings of healthiness ($t(26) = -5.28$; $P < 0.001$; 95% CI, 17.1–38.93) (**g**) and frequency of consumption ($t(26) = -4.03$; $P < 0.001$; 95% CI, 5.55–17.11) (**h**) differed between conditions. Each dot represents the mean for that food (28) from $n = 52$ participants; error bars, s.e.m. *$P < 0.05$; all tests are two-tailed.

metabolic outcomes, total grams of each macronutrient and %kcal from UPFs were entered as covariates and found to have no effects. Jointly, these findings suggest that degree of food processing alters post-ingestive metabolic rate dynamics, and compared to a nutritionally matched non-UPF meal, the UPF meal blunts the post-ingestive shift from fat to carbohydrate oxidation. The attenuated post-ingestive increase in carbohydrate oxidation observed in the UPF condition may also contribute to the increased insulin response.

Associations between metabolic and brain responses

Prior evidence suggests that post-ingestive metabolic signals are associated with, and are hypothesized to shape, the learned value of food through gut-to-brain signalling and repeated exposure[12,13,20]. We selected foods for the picture set that are generally familiar and frequently consumed across the population, as confirmed in our validation study[21] and in our current population (Fig. 3). We reasoned that the metabolic effects of these foods would be well-learned through exposures before participation in this research study, as prior studies using food picture sets and fMRI paradigms have demonstrated[10,11,22]. Therefore, we sought to examine whether post-ingestive metabolic responses were associated with food-cue reactivity, a measure of brain response to food pictures that relies on the learned subjective value of food. To test this hypothesis, participants included in the analysis of metabolic variables also completed a Becker–DeGroot–Marschak (BDM) auction task during fMRI on a separate day; notably, the non-UPF and UPF meals used in the metabolic sessions were derived from a ~300 kcal subset of the foods used in the BDM task. To examine the relationship between metabolic responses and food-cue reactivity, we focused on the picture-viewing period by bringing the first-level non-UPF > UPF contrast for the 5 s picture-viewing epoch forward to the group-level analysis. We also calculated the difference in peak metabolic change between conditions (non-UPF − UPF). Prior work in both humans and rodents has shown that peak metabolic responses to sugar-sweetened beverages are associated with striatal activation[15,16,23]; therefore, we examined both whole-brain-corrected and small-volume-corrected results within an a priori striatal mask (see Methods for details; Supplementary Fig. 2).

Immediately before and after the fMRI session, participants rated hunger, fullness and thirst (Extended Data Fig. 4). Pre-scan hunger ratings were relatively neutral ($M = 56.46$) and increased modestly to a post-scan mean of 70.00 ($t(51) = 4.69$; $P < 0.001$; 95% CI, −19.34 to −7.74). Thirst ratings showed a similar pattern, rising from a pre-scan mean of 53.23 to 63.96 post-scan ($t(51) = 4.98$; $P < 0.001$; 95% CI, −15.06 to −6.4). As expected, fullness decreased over the session ($t(51) = -4.70$; $P < 0.001$; 95% CI, 5.64–14.05).

Regressing the between-condition change in peak carbohydrate oxidation on participant-level non-UPF > UPF contrast estimates revealed a whole-brain family-wise error (FWE)-corrected association in the left superior temporal gyrus ((−44, −24, −8); $t = 7.33$; $P_{FWE} = 0.013$; Fig. 2b and Extended Data Table 2). Within our a priori striatal mask, small volume correction (SVC) identified significant associations in the right caudate ((6, 10, 4); $t = 6.11$; SVC $P_{FWE} = 0.007$; Fig. 2c and Extended Data Table 2), and the left ventral striatum ((−8, 6, −10); $t = 5.20$; SVC $P_{FWE} = 0.045$; Fig. 2d and Extended Data Table 2). Specifically, a larger increase in peak carbohydrate oxidation for non-UPF relative to UPF was negatively associated with the neural response (non-UPF > UPF) (Fig. 2b–d and Extended Data Table 2). As expected, given the close correspondence between these measures, peak RER exhibited a similar relationship in the left superior temporal gyrus ((−44, −24, −8); $t = 7.63$; $P_{FWE} = 0.007$) and SVC right caudate ((4, 8, 2); $t = 5.77$; SVC $P_{FWE} = 0.014$; Fig. 2e and Extended Data Table 2). In addition, peak RER was also associated with a second locus of activation in the right caudate ((22, −12, 24); $t = 5.48$; SVC $P_{FWE} = 0.026$; Fig. 2f and Extended Data Table 2). Between-condition changes in peak metabolic rate, fat oxidation, blood glucose and blood insulin were not significantly associated with neural responses. Together, these findings are consistent with the possibility that a food processing-related shift in post-ingestive carbohydrate oxidation may be associated with

food-cue reactivity, learned through exposure to these foods, extending previous findings from beverages to whole foods and providing additional evidence consistent with pre-clinical findings that carbohydrate metabolism is important for neural response[15,16,23].

Hunger, fullness and thirst changed significantly over the session; therefore, we explored additional models of all fMRI findings with these factors entered as covariates and found the pattern of results unchanged (Supplementary Tables 1–4). The results also remained similar after adjustment for BMI (Supplementary Table 5). Age and sex were included as covariates in all models.

Willingness to pay and brain correlates of subjective value

We next evaluated processing-related differences in subjective food value in the full fMRI cohort ($n = 52$). First, to identify attributes of the food picture set that could influence valuation, participants rated the food image set on liking, frequency of consumption, familiarity, expected satiety, perceived healthiness, estimated energy density and estimated calories before the fMRI scan, and provided estimated price ratings after the scan so as to not influence bidding behaviour during the scan. Notably, the food image set was designed and validated on an independent out-of-sample cohort to be matched on these rated attributes, nutritional properties and visual properties of the picture stimuli[21] (Supplementary Fig. 1). All attributes except perceived healthiness were rated similarly between non-UPF and UPF foods[21].

Consistent with the prior validation[21], ratings did not significantly differ for estimated calories ($t(26) = 0.99$; $P = 0.33$; 95% CI, −51.55 to 18.08; Fig. 3a), estimated energy density ($t(26) = -1.21$; $P = 0.24$; 95% CI, −23.28 to 90.03; Fig. 3b), estimated price ($t(26) = -0.35$; $P = 0.73$; 95% CI, −0.43 to 0.61; Fig. 3c), liking ($t(26) = -0.46$; $P = 0.65$; 95% CI, −6.29 to 9.89; Fig. 3d), expected satiety ($t(26) = -1.99$; $P = 0.06$; 95% CI, −0.37 to 21.28; Fig. 3e) or familiarity ($t(26) = -0.09$; $P = 0.93$; 95% CI, −5.31 to 5.79; Fig. 3f). As in the previous study, participants rated non-UPF as healthier than UPF ($t(26) = -5.28$; $P < 0.001$; 95% CI, 17.1–38.93; Fig. 3g). Unexpectedly, frequency of consumption also differed by processing category in this sample ($t(26) = -4.03$; $P < 0.001$; 95% CI, 5.55–17.11; Fig. 3h), with non-UPF rated as being consumed more often than UPF. Therefore, we adjusted for healthiness and frequency of consumption by adding it as a trial-by-trial parametric modulator or covariate in subsequent models comparing UPF to non-UPF.

To quantify subjective food value, participants completed a BDM auction task concomitant with fMRI. During the task, participants viewed all 28 food images and bid their willingness to pay (WTP; $0–$5) for each item (see Methods and Fig. 2a). The measure of WTP, while adjusting for perceived healthiness and frequency of consumption in the model, did not differ between the non-UPF and UPF conditions ($t(32.41) = 0.96$; $P = 0.34$; Fig. 4a and Supplementary Table 6). When sex was entered as a covariate in the model, the results were unchanged.

Although WTP did not differ by processing category, we next tested whether processing level could modulate the neural representation of subjective value by entering WTP as a parametric modulator. Consistent with prior work, measures that differed by condition were included as additional parametric modulators[10,22]; in our case, these were frequency of consumption and perceived healthiness, as the photo set did not differ by condition in nutritional or visual property measures.

First, as a check of our procedures, we examined the WTP model regardless of condition. Consistent with meta-analysis findings from BDM auction tasks[24], WTP was associated with activation in the left orbitofrontal cortex ((−28, 24, −34); $t = 6.27$; $P_{FWE} = 0.001$; (−24, 30, −20); $t = 5.78$; $P_{FWE} = 0.005$; Fig. 4b) and the left pregenual anterior cingulate cortex ((−14, 52, 4); $t = 5.40$; $P_{FWE} = 0.021$; (−6, 52, 2); $t = 5.20$; $P_{FWE} = 0.043$). WTP-related activity was also observed in regions implicated in higher-order visual processing, including the right fusiform gyrus ((46, −62, −14); $t = 5.64$; $P_{FWE} = 0.008$) and the right lateral occipital cortex ((44, −78, −6); $t = 5.50$; $P_{FWE} = 0.014$). A complete list of activations is provided in Extended Data Table 2.

Next, we tested whether activity was associated differently across UPF versus non-UPF conditions, while adjusting for frequency of consumption and perceived healthiness. Peak differences were observed in the left occipitotemporal gyri, specifically the left fusiform gyrus ((−32, −52, −14); $t = 7.89$; $P_{FWE} < 0.0001$; Fig. 4c and Extended Data Table 2) and two peaks in the left lingual gyrus ((−22, −84, −14); $t = 7.32$; $P_{FWE} < 0.0001$; (−24, −74, −8); $t = 6.69$; $P_{FWE} = 0.0001$; Fig. 4d and Extended Data Table 2). Parameter estimates of the left fusiform gyrus and the left lingual gyrus indicated opposing responses, with positive associations with value in the non-UPF condition and negative in the UPF condition (Fig. 4c,d and Extended Data Table 2). We next examined effects within our single a priori striatal mask using an SVC. This analysis revealed significant activation in the right putamen ((32, −4, 12); $t = 4.62$; SVC $P_{FWE} = 0.017$; Fig. 4e) and in the right caudate ((14, 16, 4); $t = 4.34$; SVC $P_{FWE} = 0.043$; Fig. 4f and Extended Data Table 2). Both regions showed a similar pattern to the activation in the occipitotemporal gyri, with positive parameter estimates—and therefore a positive correlation between brain activity and bid value—for non-UPF cues and negative parameter estimates—indicating a negative correlation—for UPF cues (Fig. 4e,f). Interestingly, the contrast UPF > non-UPF did not yield any significant voxels at either the whole-brain or SVC level. Collectively, WTP did not differ between non-UPF and UPF conditions, even after controlling for frequency of consumption and perceived healthiness (Supplementary Table 6); however, neural differences were still observed. This could reflect differences at the individual level in how subjective value is encoded in these foods despite no overall group difference in bidding behaviour.

Although our stimuli were matched on nine visual properties, we further explored a model accounting for trial-by-trial variation in visual properties (complexity and object size) of our stimuli and found they did not alter the pattern of results (Supplementary Table 5).

Discussion

Here, we provide evidence that UPFs may influence metabolic and learned neural responses differently from nutrient-matched non-UPFs. First, we demonstrated that even when meals were matched across multiple nutritional factors, the degree of food processing classified by Nova significantly altered post-ingestive metabolic responses. Next, we showed that these metabolic differences were associated with neural responses to non-UPF versus UPF food cues. Finally, although behavioural indices of subjective value did not differ between non-UPF and UPF, the neural representation of subjective value did, with condition-dependent value signals observed in higher-order visual and striatal regions. Taken together, these findings provide experimental evidence that Nova processing level may influence post-ingestive metabolic responses and, in turn, the neural response to food cues in ways not explained by macronutrient composition alone, supporting the hypothesis that altered nutritional availability is a candidate mechanism linking UPF consumption to metabolic health and overeating[5,13,20].

Food processing can modify post-ingestive physiology, often by increasing carbohydrate availability and elevating glycaemic index, thereby producing larger postprandial blood glucose and insulin responses[7,8]. Prior work has reported differences in metabolic rate and respiratory quotient following meals differing in degree of processing; however, these effects are difficult to attribute directly to processing, as the test meals also differed in total energy and macronutrient composition[25]. The present findings address this limitation directly: the test meals were matched on energy, macronutrients and glycaemic index and yielded comparable blood glucose AUC, while the UPF condition elicited larger insulinaemic and energetic responses with attenuated carbohydrate oxidation. Notably, homogenized meals can produce similar blood glucose responses to their intact counterparts while altering other postprandial metabolic responses[26], paralleling the pattern

https://doi.org/10.1038/s42255-026-01619-4

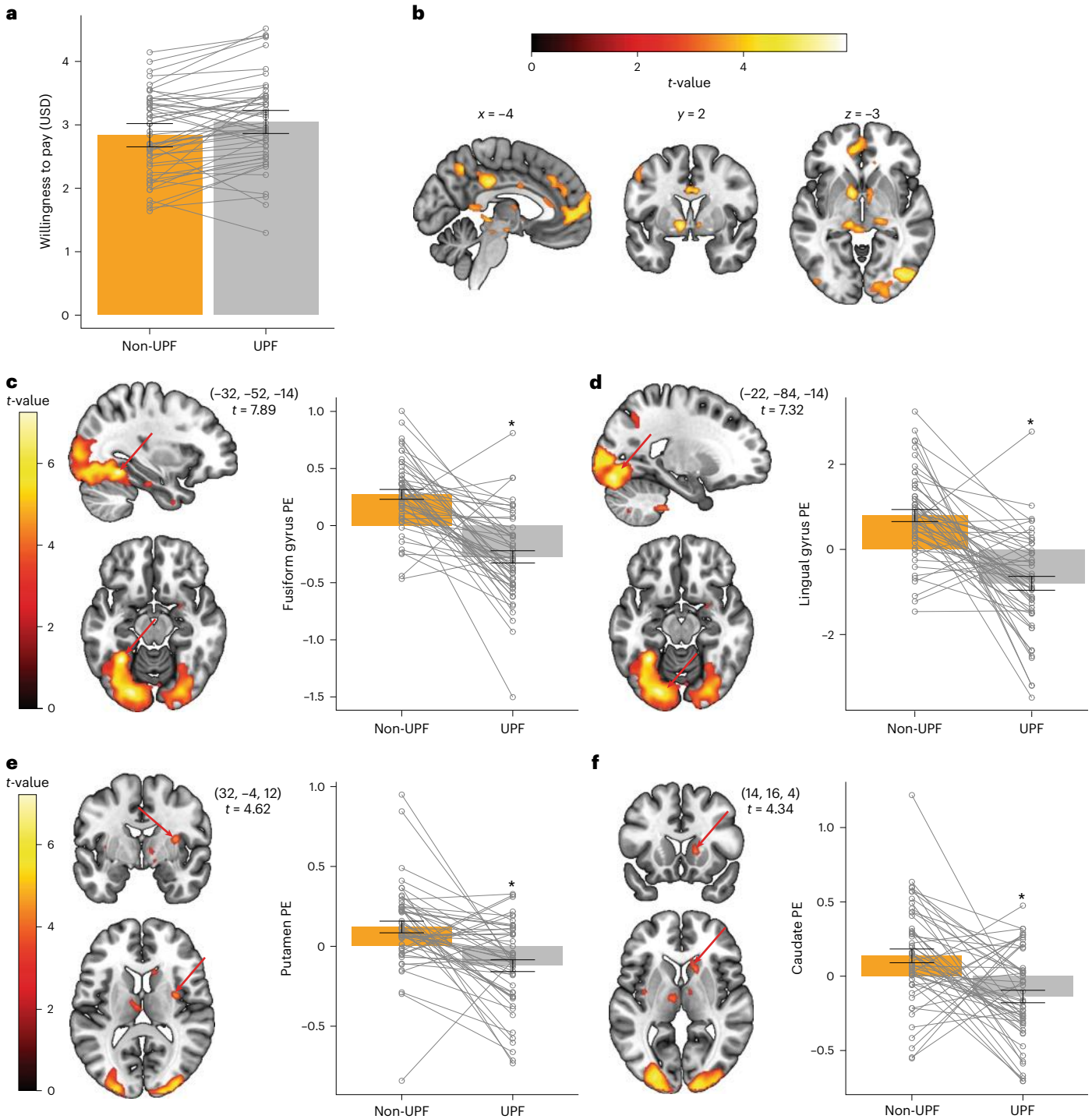


Fig. 4 | Food value is associated with brain response. a, Participants bid similar amounts for non-UPF and UPF pictures after controlling for frequency of consumption and healthiness ($t(32.41) = 0.96$; $P = 0.34$). **b**, Overall value, as measured by willingness to pay for each food item, was associated with activity in brain areas consistent with prior work using the BDM auction task. **c**,**d**, In a whole-brain analysis, value for non-UPF items was positively associated with activity in the fusiform gyrus ((−32, −52, −14); $t = 7.89$; $P_{FWE} < 0.00010$) (**c**) and lingual gyrus ((−22, −84, −14); $t = 7.32$; $P_{FWE} < 0.0001$) (**d**), whereas value for UPF items was negatively associated with activity in these same regions. **e**,**f**, In an a priori ROI analysis, value was again oppositely associated with non-UPF versus UPF items in the putamen ((32, −4, 12); $t = 4.62$; SVC $P_{FWE} = 0.017$) (**e**) and caudate ((14, 16, 4); $t = 4.34$; SVC $P_{FWE} = 0.043$) (**f**). Arrows point to the significant FWE-corrected peak displayed within a cluster threshold of $P_{uncorrected} < 0.001$. Each dot represents a participant; error bars, s.e.m. $n = 52$ participants. *$P < 0.001$; tests are two-sided.

observed across our conditions. Importantly, many UPF products, despite being eaten as solids, are formulated to transition quickly into a lubricated, semi-fluid bolus. For brittle snacks and cereals, processing promotes extensive first-bite fracturing and rapid saliva incorporation, while added lipids increase lubrication, together facilitating faster, more homogeneous bolus formation[27]. These manufacturing techniques are primarily intended to optimize the oral sensory experience; however, they may unintendedly also influence digestion kinetics and downstream metabolic responses, such as the observed higher insulinaemic response but similar peak blood glucose levels, a

pattern consistent with a relative reduction in insulin sensitivity. We also observe a potential delayed shift in substrate oxidation, which is also observed in insulin resistance and type 2 diabetes[28,29]. Although this study was not designed to assess chronic outcomes, the present data show that nutrient-matched non-UPF and UPF meals elicit acutely different post-ingestive glycaemic and insulinaemic responses and alter substrate oxidation, suggesting a plausible physiological mechanism through which repeated exposures could contribute to the metabolic dysfunction reported in epidemiological studies[4,5].

These metabolic differences may also shape neural responses to food cues. Post-ingestive metabolic signals are a key reinforcing stimulus linking orosensory food cues to their nutritional value[12,14], and these signals are thought to be integrated in the striatum (both dorsal and ventral) and guide eating behaviour[13,20]. This gut-to-brain signalling is thought to be macronutrient specific, with fat signalling through PPARα (peroxisome proliferator-activated receptor alpha) receptors on the vagus nerve[19]. Although carbohydrate sensing has multiple proposed mechanisms, including activation of the sodium-glucose transporter[14], vagal and spinal afferent-dependent pathways[17,18] and an unknown carbohydrate oxidation sensor[23], insulin secretion is not macronutrient specific and can be evoked by carbohydrates and proteins. In animal models, there is some evidence that it influences food preference[30], and in humans, intranasal inulin increases response to sweet tastes[31]. Although we observed differences in multiple metabolic measures, our data provide additional evidence for the importance of carbohydrate oxidation in conveying nutrient information to the brain.

Although we replicate previous findings that carbohydrate oxidation is associated with ventral striatal activation, the direction of the relationship differs. Notably, the other studies reported a positive association between post-ingestive metabolic responses and striatal activation[15,16]. This discrepancy may reflect a key methodological difference: prior studies measured neural responses during oral flavour receipt, whereas the present study assessed responses to visual food cues, which have been shown to evoke distinct and sometimes opposite neural responses[32]. However, we do replicate the finding that peripheral post-ingestive metabolic signals are associated with striatal activation, although previous studies[15,16], including the present one, differ in which specific metabolic signal drives this relationship. This heterogeneity may reflect the fact that these multiple metabolic measures could index a shared underlying metabolic process. Overall, we provide evidence for the framework in which differences in nutrient availability can guide eating through learning[12,13,20].

In addition to striatal regions, processing-related individual differences in carbohydrate oxidation were also associated with responses in the superior temporal gyrus (STG). Although primarily known for its role in auditory and language processing, the STG is also responsive to food cues[33]. More work is needed to determine whether the STG is involved in food-specific multisensory integration, including interoceptive metabolic signals.

The subjective value of food as measured by our auction task did not differ between conditions, which is consistent with the meals being matched with respect to energy density and macronutrient composition, attributes that have previously been shown to drive differences in subjective food valuation[10,11,22], but was contrary to our hypothesis. Although we did not find large differences in subjective food value across processing, differences in the neural encoding of subjective food value were observed. Notably, prior work has shown that the subjective value of foods high in both fat and sugar, relative to foods high in either nutrient alone, is associated with different activity in the putamen and caudate[10], and although our conditions were matched in macronutrient composition, we observed a similar pattern of striatal activation, suggesting that processing level, and potentially nutrient availability, may engage these regions through mechanisms independent of macronutrient content.

Interestingly, we observed condition differences in subjective value associations in the occipitotemporal gyrus, specifically the fusiform and lingual gyri. Although the fusiform gyrus is best known for its role in face processing within the ventral visual stream, a distinct region identified for food-specific visual processing has also been found and termed the fusiform food area[34]. Response in the fusiform food area is modulated by circulating glucose, insulin and ghrelin[35,36]. The lingual gyrus has been reported in studies of food cues[37], and the visual association cortex in mice can be sensitive to reward associations[38].

Limitations and future directions

There are a few limitations that should be acknowledged in this work. First, we assembled the test meals from a diverse set of foods to ensure that metabolic responses were not driven by any single item. Although total protein was matched, the sources of protein in each meal differed and could have influenced insulin response[39]. Second, inherent in the Nova definition are additives and alterations in the food matrix; the UPF meal contained more additives, and we did not explicitly measure physical and chemical structures of foods comprising the food matrix, beyond total fibre. Third, responses may also differ to larger caloric loads. Additional tests of these factors will be important to establish the generalizability of these findings. Fourth, prior work indicates that UPFs are consumed more rapidly under ad libitum conditions[25,40]. By contrast, in the present study, the meals were isocaloric (~300 kcal) and fully consumed, and the non-UPF meal was eaten slightly faster than the UPF meal. However, the modest 1.5 min difference in eating time is unlikely to produce a physiologically meaningful effect[41]. Finally, WTP did not differ between conditions. Local grocery prices changed rapidly during the time of data collection; future studies should explicitly collect fluctuating food prices.

Conclusions

In summary, we provide evidence that non-UPF and UPF meals matched across a variety of nutritional factors elicit distinct post-ingestive metabolic responses, specifically amplified insulinaemic and energetic responses with attenuated carbohydrate oxidation after UPF consumption. These processing-related metabolic differences were also associated with neural metrics of food-cue reactivity within the striatum across foods that differ in degree of processing. Collectively, these findings support the concept that food processing could influence physiology and brain function through mechanisms extending beyond calories and macronutrient composition alone, while identifying altered nutritional availability from altered physical structure as a plausible contributor to both their overconsumption and effects on metabolic health.

Methods

General study overview

All study protocols were approved by the Virginia Tech Institutional Review Board (21-1052) and registered at ClinicalTrials.gov (identifier: NCT06017986). The study consisted of a pair of metabolic sessions, a behavioural session and an fMRI session. The two metabolic sessions were held on separate days in a randomized crossover design to test whether degree of processing alters postprandial metabolic response independent of nutrient content. During each session, participants resided in a whole-room indirect calorimeter for 4 h and consumed a nutritionally matched non-UPF or UPF meal. A 50 min baseline measurement and blood draw were collected before meal consumption, followed by 3 h of postprandial metabolic measurements and serial blood draws to characterize postprandial metabolic responses to UPF versus non-UPF meals. As these sessions had a high participant burden, we completed them in a subset ($n = 32$) of the total ($n = 57$) sample.

In the behavioural session, anthropometric measures were collected, and participants were trained on the rating scales before rating 28 food images (14 non-UPF and 14 UPF). In the fMRI session,

participants completed four runs of a BDM auction task during fMRI acquisition to quantify food value and test whether valuation-related brain responses differed as a function of processing level for the same 28 images presented in the behavioural session.

Picture stimuli

For this study, a picture set of 28 foods that are commonly consumed in the United States but systematically differ in degree of processing was used. As previously reported, using the Nova classification system[5], the picture set was divided into two groups differing in the degree of processing: 14 non-UPFs (Nova 1–3) and 14 UPFs (Nova 4). To verify that the food picture set was Nova-scored correctly, 67 raters, including 17 registered dietitians, Nova-scored the picture set and showed strong inter-rater reliability, as reported in a prior publication[21]. These foods were additionally matched on 26 characteristics consisting of nine visual properties (for example, pixel colour, object size and brightness), 11 nutritional characteristics (for example, calories, energy density and macronutrients) and six perceptual properties (for example, perceived liking, estimated energy density, estimated cost and expected satiation)[21].

Meal stimuli

The non-ultraprocessed and ultraprocessed meals used in the metabolic sessions were derived from a 300 kcal subset of the 28 foods used in the picture set[21]. The nutritional information for all 28 foods was derived from the Nutrition Data System for Research (version 2022) and then entered into an algorithmic process of testing combinations of different food pairings with different portion sizes to identify the most nutritionally matched set of non-UPF and UPF meals. Through this process, the final non-UPF and UPF meals were matched on weight, energy, energy density, total carbohydrates, total fats, total proteins, available carbohydrates, glycaemic index, glycaemic load, total dietary fibre, sodium and water, all with <1.6% error between meals. To match weight, energy, energy density and water, a 12 g serving of water was added to the UPF meal. Nutritional information and a list of the foods are available in Fig. 1b.

Recruitment and screening

Study participants were recruited from the university and surrounding community in Roanoke, Virginia, through social media advertisements, campus advertisements and flyers. Interested individuals filled out a general online screening form on Ripple Science software from June 2023 to December 2025 to provide self-report information for the determination of study eligibility. To be eligible, individuals had to be between 18 and 45 years old with a BMI between 18.5 and 25 (calculated from reported height and weight). Exclusion criteria included having dietary restrictions (food allergies, vegetarian, keto and so on), medical conditions (including metabolic, neurologic or psychiatric disorders) or medications used to treat these disorders; being pregnant; currently using inhaled nicotine or recreational drugs other than periodic cannabis use; having impaired taste or smell; having contraindications for MRI; or having vision not sufficiently correctable to see the MRI screen. Eligible individuals were invited for in-person screening and consent. Data collection started in June 2023 and ended in December 2025, and the metabolic sessions spanned June 2023 to March 2025. Participants were compensated for their time.

Statistics and reproducibility

Power analysis (behaviour). The overall sample size was estimated based on behavioural data from a previous publication[10]. Sample size was calculated in R[42] based on a repeated-measures ANOVA model, and detecting differences in WTP (bid amount in USD) among the degree of food processing condition groups[43]. With a total sample size of 52 participants, pairwise comparisons among the two groups yielded 80% power to detect an effect size of Cohen's $f = 0.40$ with a type I error rate of 5%. Based on this total sample size of 52, power was estimated for a generalized linear mixed-effects model, regressing the primary outcome (WTP) on food processing, sex, their two-way interaction and controlling for potential confounders (hunger, energy expenditure, blood glucose, blood insulin). This was accomplished using 5,000 iterations of a Monte Carlo simulation; expected assumptions were based on published bidding data[10]. In these simulations, the model parameters were estimated by restricted maximum likelihood, such that the specified model was compared to the null model using the likelihood ratio test, yielding 99% power to detect a statistically significant effect at the 5% level of significance. In summary, a sample size of 52 participants provides sufficient power to detect a main effect difference in WTP by food processing group.

Power analysis (associations between metabolism and fMRI). An ad hoc power analysis was conducted to ensure that power was achieved for the subset of participants in the correlations between metabolic and brain responses. The most relevant published data[16] reported a correlation of $r = 0.83$, substantially exceeding the effect sizes used to power the study. We performed a power analysis based on a test of Pearson's correlation with that value. To achieve 95% power, 16 participants were needed at a significance level of 0.0001.

Power analysis (metabolism). A separate power analysis was conducted to evaluate the sample size needed to detect a difference in metabolic response to the meals consumed in the whole-room indirect calorimeter. There was over 80% power to detect a difference, based on a paired *t*-test, in the AUC for energy expenditure, assuming a Cohen's *d* of 0.57 (medium size) and a sample size of 27. Data collection and analysis were not performed blind to the conditions of the experiment.

Participant inclusion and eligibility

Study-wide participant inclusion and exclusion are presented in a CONSORT diagram (Extended Data Fig. 1). A total of 61 participants completed in-lab eligibility screening. Four participants were excluded before enrollment (two were ineligible for the study payment system and two were not interested). The remaining 57 participants enrolled, and all completed the fMRI session. Five participants were subsequently excluded from the fMRI analyses: two because of excessive head motion (>2 mm in more than two of the four runs), two because of task performance (>25% of bids <$0.25 or missing) and one because of equipment failure. Of the 52 participants included in the fMRI analyses, four had one run excluded, two were excluded because of excessive head motion and two were excluded because of equipment failure. Two additional participants were missing two runs; one because of excessive head motion and one because of equipment malfunction.

Of the 57 enrolled participants, 32 completed the metabolic sessions. All participants completed both the non-UPF and UPF conditions; however, one participant experienced a vasovagal response after the 60 min blood draw, resulting in early termination of that session. Owing to IV patency issues, glucose samples could not be obtained for one condition in five participants. Insulin samples could not be obtained for one condition in three participants and for both conditions in one participant. All 32 participants who completed the chamber sessions also underwent MRI scanning: two were excluded because of excessive head motion (>2 mm in more than two of the four runs) and one because of equipment failure.

Missing data from metabolic sessions

There was minimal missing data across the study. Data were analysed using linear mixed-effects models, which allow for unequal observations per participant (Supplementary Materials).

Anthropometric

Body weight was measured with an electronic scale (Health O Meter ProPlus digital scale), and height was measured with a wall-mounted

stadiometer. Weight was recorded to the nearest 0.1 kg and height to the nearest 1 cm. BMI was calculated as kg m^{-2}. Waist and hip circumference were measured using a Gulick tape measure following World Health Organization protocols for the calculation of waist-to-hip ratio.

Habitual diet

Information on habitual diet measures can be found in the Supplementary Materials.

Metabolic session

Participants completed two separate metabolic sessions on different days in a randomized crossover design. To reduce participant burden, we did not require a specific session spacing. Seven participants had sessions within 3 days, 14 participants had sessions between 4 days and 2 weeks, seven participants had sessions between 15 days and 4 weeks and four participants had sessions with a greater than 4-week gap. For each session, participants were instructed to arrive after an overnight fast and to refrain from strenuous exercise on the preceding day. Sessions were scheduled to begin in the morning, after participants' habitual wake-up time. A small-volume whole-room indirect calorimeter (MEI Research) was used to measure participants' metabolic rate, RER, carbohydrate oxidation and fat oxidation for 4 h (ref. 44). More details on chamber configuration can be found in the Supplementary Materials.

After arrival and entry into the whole-room indirect calorimeter, participants completed a 50 min baseline measurement. The average of the 15 min before test meal consumption (minutes −30 to −15) was used as the baseline to ensure a stable reference for calculating change from baseline. At minute 50, without disrupting the whole-room indirect calorimeter, participants uncovered and then consumed the test meal in under 10 min. After meal consumption, the postprandial metabolic response was measured for 3 h. Concomitant with the indirect calorimeter measurement, blood draws were performed at baseline (60 min before meal consumption) and after meal consumption at minutes 5, 20, 40, 60, 90, 120 and 180. Blood draws were performed through custom ports so as not to disturb the WRIC measurements. For blood sample analyses, glucose concentrations were measured in duplicate using a point-of-care system (HemoCue Glucose 201 System), insulin concentrations were quantified using an enzyme-linked immunosorbent assay (ALPCO) and haemoglobin A1c was determined with a point-of-care analyser (Afinion HbA1c, Abbott Laboratories). Throughout the metabolic session, participants were also fitted with accelerometers (ActiGraph wGT3X-BT) on their right wrist and left ankle to measure movement. Internal states (hunger, fullness and thirst) were assessed before and after the WRIC measurements, as well as immediately after meal consumption and 60 min after the meal. During the post-meal measurement, participants also rated the meal for perceived liking using the labelled hedonic scale, and wanting on a visual analogue scale.

Behavioural session

All ratings were collected using PsychoPy3 (v.2023.1.0)[45]. Before providing liking ratings, participants completed training on proper use of the labelled hedonic scale[46] and practised rating a variety of remembered sensations. Following this training, participants rated an example food image (not included in the 28-food picture set) to practise the full set of ratings (liking, frequency of consumption, familiarity, expected satiety, perceived healthiness, estimated energy density and estimated calories) before assessing all 28 foods (Supplementary Materials).

At the end of the behavioural session, all participants practised a run of the fMRI task (described below) in a mock MRI simulator (Psychology Science Tools) equipped with a mock 64-channel head coil.

fMRI session

Participants were instructed to arrive neither hungry nor full, having fasted for 3 h, and to refrain from strenuous exercise the day before. In relation to the metabolic sessions, six participants completed the fMRI session as their last session, seven participants completed the fMRI session between their metabolic sessions and 16 participants completed the fMRI session before their metabolic sessions. During this session, participants completed four runs of a BDM auction task to assess food value[47] while undergoing fMRI scanning[24]. Additional details can be found in Supplementary Materials.

Immediately before and after scanning, participants rated their hunger, fullness and thirst. Ratings were made on visual analogue scales anchored with 'not hungry at all' to 'very hungry', 'not full at all' to 'very full' and 'not thirsty at all' to 'very thirsty'. After completing the fMRI scan, participants rated the estimated price of each of the 28 foods using the same rating scale as in the scanner. This assessment was administered post-scan to avoid biasing bidding behaviour during the task.

MRI acquisition parameters

All MRI data were acquired with a 3 Tesla Siemens MAGNETOM Prisma scanner using a 64-channel head coil. Acquisition parameters for the functional echo-planar images were TE = 34 ms, echo spacing = 0.66 ms, TR = 1.5 s, flip angle = 70, voxel size = 2 × 2 × 2 mm, number of slices = 72 and multiband acceleration factor = 4. To allow distortion correction, sets of identical images were acquired with reverse-phase (posterior-to-anterior and anterior-to-posterior) encoding polarity. A high-quality T1-weighted anatomical image (TE = 2.32 ms, TR = 2.3 s, flip angle = 8, slices = 192, field of view = 240 mm, voxel size = 0.9 × 0.9 × 0.9 mm) was acquired for registration of functional images.

Data analysis

Metabolic analysis. All statistical analyses on metabolic data were conducted with R version 4.4.1 (2024-06-14). Internal state ratings before and after the metabolic measurements, as well as immediately after meal consumption and 60 min after the meal, were compared using linear mixed-effects models with internal state (hunger, fullness or thirst) as the outcome, time as a fixed effect and participant as a random intercept. In addition, post-meal liking and wanting ratings were compared across the non-UPF and UPF conditions using linear mixed-effects models. In these models, condition was included as a fixed effect and random intercept for participant to account for within-subject correlations. Where multiple comparisons were performed, appropriate corrections were applied.

Baseline measures were compared across conditions to check for any systematic differences. Baseline measures included resting metabolic rate, resting RER, resting carbohydrate oxidation, resting fat oxidation, baseline blood glucose, baseline blood insulin and pre-meal movement AUC, calculated as the summed ActiGraph arm and leg movement signals. These outcomes were compared across the non-UPF and UPF conditions using linear mixed-effects models. In these models, condition was included as a fixed effect and a random intercept for participant to account for within-subject correlations.

Blood outcomes of interest included AUC of change from baseline in insulin and glucose levels. Each of these outcomes was compared across the non-UPF and UPF conditions using linear mixed-effects models. In these models, condition was included as a fixed effect and a random intercept for participant to account for within-subject correlations. Additionally, each insulin and glucose measure at each of the eight time points was examined using a linear mixed-effects model with fixed effects of time, condition and a time-by-condition interaction. A random intercept for participant was included to account for within-subject correlation. Two-sided post hoc Wald-type tests were conducted to examine differences between time points. Holm–Bonferroni correction was used to control the FWE rate.

WRIC outcomes of interest included AUC of change from baseline in metabolic rate, RER, carbohydrate oxidation and fat oxidation. Each

of these four outcomes was compared across the UPF and non-UPF conditions using linear mixed-effects models. In these models, condition was included as a fixed effect and a random intercept for participant to account for within-subject correlations.

For each model, residuals were visualized, and assumptions of normality and homoscedasticity were determined to be met.

Behavioural analysis. All statistical analyses on behavioural data were conducted with R version 4.4.1 (2024-06-14). Where multiple comparisons were performed, appropriate corrections were applied. All tests were two-sided. To test whether the average estimated price, liking, perceived healthiness, familiarity, perceived satiety and frequency of consumption were different across non-UPF and UPF foods, linear regression models were used. In these models, the dependent variable was the mean rating for each food (averaged across participants) for each outcome, and food type (non-UPF vs UPF) was the independent variable[10,11,22]. To examine differences in WTP, linear mixed-effects models were performed with WTP as the outcome and food type as the fixed effect. Perceived healthiness and frequency ratings were entered as covariates, as they differed between conditions. Random intercepts for food item and participant, as well as a random slope for food type within participant, were included to account for any within-subject or within-food correlations. This covariance structure was selected using Akaike's information criteria. For each model, residuals were visualized, and assumptions of normality and homoscedasticity were determined to be met.

fMRI analyses. Internal state ratings pre-MRI and post-MRI session were compared using linear mixed-effects models with internal state (hunger, fullness or thirst) as the outcome, time (pre or post) as a fixed effect and participant as a random intercept.

fMRI data were preprocessed with FSL version 6.0.7.17 (FMRIB Software Library) and SPM version 25.01.02 (Statistical Parametric Mapping) implemented in MATLAB R2021b. Susceptibility-induced distortions were estimated using opposite phase-encoded images and corrected with a Jacobian transformation using FSL[48] topup[49]. Preprocessing was then completed with SPM and included realignment, coregistration of the functional images to each participant's T1-weighted anatomical image, spatial normalization to standard space and spatial smoothing with a 6 mm full-width half-maximum Gaussian kernel.

First and group-level models. Two first-level general linear models (GLMs) were specified. For both GLMs, the interval from the onset of the post-picture fixation period through bid submission (that is, the participant-specific reaction time during each bidding period) was modelled as a regressor of no interest. Additional fMRI analysis information can be found in the Supplementary Information.

The first GLM was designed to capture food-cue reactivity by modelling the 5 s picture-viewing period with a boxcar regressor, with separate regressors for non-UPF and UPF trials[10,22]. For the first GLM, the non-UPF > UPF contrast was brought to the group level and used to test the association with the between-condition difference in peak metabolic response to the test meals (non-UPF − UPF) measured during the metabolic sessions. To determine the peak metabolic response, we identified local maxima as time points exceeding their immediately preceding and following values. Candidate peaks were retained if their magnitude was at least 75% of the subsequent local maximum and if they occurred at least four units earlier. The peak metabolic response was defined as the first local maximum that met these criteria. Separate models were estimated for each metabolic measure (carbohydrate oxidation, RER, metabolic rate, fat oxidation, blood glucose and blood insulin). No additional correction for multiple comparisons across metabolic measures was applied, as each represented an a priori physiological outcome of interest and was evaluated independently, consistent with previous studies examining metabolism–brain associations[15,16].

For the second GLM that examined value, group-level analyses assessed value-related activity by examining the WTP parametric modulator during picture viewing and testing differences in value-related responses between the non-UPF and UPF cues. The second GLM was designed to capture value-related responses while accounting for measures that differed across conditions (frequency of consumption and perceived healthiness), such that effects attributed to food type were not confounded by these factors. Accordingly, the second model was identical to the first but additionally included trial-wise WTP, frequency of consumption and perceived healthiness as parametric modulators of the 5 s picture-viewing regressor. The contrast of non-UPF > UPF and UPF>non-UPF was then tested on the second level to examine the interaction, or the difference, between the association of WTP across UPF and non-UPF items.

Prior work has shown that peak metabolic responses are associated with striatal activation[15,16], and recent meta-analyses have also associated the striatum with differences in WTP[24]. Accordingly, we examined both GLMs using whole-brain corrected analyses and SVC within a single a priori striatal mask (caudate, putamen and nucleus accumbens) derived from the Harvard–Oxford atlas[50]. These regions were extracted bilaterally using the most lenient probability threshold (largest mask), added and then binarized to create a single large mask. This single large mask was used for all region of interest analyses to reduce alpha inflation (Supplementary Fig. 2). Sex and age were entered as covariates for both GLM group-level analyses.

Corrections for multiple comparisons were applied using a peak-level FWE-corrected threshold of $P < 0.05$. For visualization of clusters containing the peak voxel, statistical maps are displayed at uncorrected $P < 0.001$, $k > 10$. Two-tailed t-tests were performed on extracted parameter estimates where appropriate.

Reporting summary

Further information on research design is available in the Nature Portfolio Reporting Summary linked to this article.

Data availability

Data underlying this manuscript are available from the Virginia Tech Data Repository (https://doi.org/10.7294/32077803)[51]. Neuroimaging data have been deposited on OpenNeuro, accession number ds007693 (ref. 52). Source data are provided with this paper.

Code availability

Code underlying this manuscript is available from the Virginia Tech Data Repository (https://doi.org/10.7294/32077803)[51]

References

1. Ravandi, B. et al. Prevalence of processed foods in major U.S. grocery stores. *Nat. Food* **6**, 296–308 (2025).
2. Williams, A. M., Couch, C. A., Emmerich, S. D. & Ogburn, D. F. Ultra-processed food consumption in youth and adults: United States, August 2021–August 2023. *NCHS Data Brief* https://doi.org/10.15620/cdc/174612 (2025).
3. Monteiro, C. A. et al. Ultra-processed foods: what they are and how to identify them. *Public Health Nutr.* **22**, 936–941 (2019).
4. Lane, M. M. et al. Ultra-processed food exposure and adverse health outcomes: umbrella review of epidemiological meta-analyses. *Brit. Med. J.* **384**, e077310 (2024).
5. Monteiro, C. A. et al. Ultra-processed foods and human health: the main thesis and the evidence. *Lancet* **406**, 2667–2684 (2025).
6. Clarke, J. D. et al. Bioavailability and inter-conversion of sulforaphane and erucin in human subjects consuming broccoli sprouts or broccoli supplement in a cross-over study design. *Pharmacol. Res.* **64**, 456–463 (2011).

7. Huang, X., Liu, H., Ma, Y., Mai, S. & Li, C. Effects of extrusion on starch molecular degradation, order–disorder structural transition and digestibility—a review. *Foods* **11**, 2538 (2022).
8. Tosh, S. M. & Chu, Y. Systematic review of the effect of processing of whole-grain oat cereals on glycaemic response. *Br. J. Nutr.* **114**, 1256–1262 (2015).
9. Cai, M. et al. Upper-gastrointestinal tract metabolite profile regulates glycaemic and satiety responses to meals with contrasting structure: a pilot study. *Nat. Metab.* **7**, 1459–1475 (2025).
10. DiFeliceantonio, A. G. et al. Supra-additive effects of combining fat and carbohydrate on food reward. *Cell Metab.* **28**, 33–44.e3 (2018).
11. Perszyk, E. E. et al. Fat and carbohydrate interact to potentiate food reward in healthy weight but not in overweight or obesity. *Nutrients* **13**, 1203 (2021).
12. Myers, K. P. The convergence of psychology and neurobiology in flavor-nutrient learning. *Appetite* **122**, 36–43 (2018).
13. de Araujo, I. E., Schatzker, M. & Small, D. M. Rethinking food reward. *Annu. Rev. Psychol.* **71**, 139–164 (2020).
14. Sclafani, A. & Ackroff, K. Role of gut nutrient sensing in stimulating appetite and conditioning food preferences. *Am. J. Physiol. Regul. Integr. Comp. Physiol.* **302**, R1119–R1133 (2012).
15. de Araujo, I. E., Lin, T., Veldhuizen, M. G. & Small, D. M. Metabolic regulation of brain response to food cues. *Curr. Biol.* **23**, 878–883 (2013).
16. Veldhuizen, M. G. et al. Integration of sweet taste and metabolism determines carbohydrate reward. *Curr. Biol.* **27**, 2476–2485.e6 (2017).
17. Fernandes, A. B. et al. Postingestive modulation of food seeking depends on vagus-mediated dopamine neuron activity. *Neuron* **106**, 778–788.e6 (2020).
18. Goldstein, N. et al. Hypothalamic detection of macronutrients via multiple gut–brain pathways. *Cell Metab.* **33**, 676–687.e5 (2021).
19. Han, W. et al. Striatal dopamine links gastrointestinal rerouting to altered sweet appetite. *Cell Metab.* **23**, 103–112 (2016).
20. Kelly, A. L., Baugh, M. E., Oster, M. E. & DiFeliceantonio, A. G. The impact of caloric availability on eating behavior and ultra-processed food reward. *Appetite* **178**, 106274 (2022).
21. Hutelin, Z. et al. Creation and validation of a NOVA scored picture set to evaluate ultra-processed foods. *Appetite* **198**, 107358 (2024).
22. Tang, D. W., Fellows, L. K. & Dagher, A. Behavioral and neural valuation of foods is driven by implicit knowledge of caloric content. *Psychol. Sci.* **25**, 2168–2176 (2014).
23. Tellez, L. A. et al. Glucose utilization rates regulate intake levels of artificial sweeteners. *J. Physiol.* **591**, 5727–5744 (2013).
24. Newton-Fenner, A. et al. Economic value in the brain: a meta-analysis of willingness-to-pay using the Becker–DeGroot–Marschak auction. *PLoS ONE* **18**, e0286969 (2023).
25. Hall, K. D. et al. Ultra-processed diets cause excess calorie intake and weight gain: an inpatient randomized controlled trial of ad libitum food intake. *Cell Metab.* **30**, 67–77.e3 (2019).
26. Peracchi, M. et al. The physical state of a meal affects hormone release and postprandial thermogenesis. *Br. J. Nutr.* **83**, 623–628 (2000).
27. Witt, T. & Stokes, J. R. Physics of food structure breakdown and bolus formation during oral processing of hard and soft solids. *Curr. Opin. Food Sci.* **3**, 110–117 (2015).
28. Corpeleijn, E., Saris, W. H. M. & Blaak, E. E. Metabolic flexibility in the development of insulin resistance and type 2 diabetes: effects of lifestyle. *Obes. Rev.* **10**, 178–193 (2009).
29. Koves, T. R. et al. Mitochondrial overload and incomplete fatty acid oxidation contribute to skeletal muscle insulin resistance. *Cell Metab.* **7**, 45–56 (2008).
30. Stouffer, M. A. et al. Insulin enhances striatal dopamine release by activating cholinergic interneurons and thereby signals reward. *Nat. Commun.* **6**, 8543 (2015).
31. Wingrove, J. et al. The influence of insulin on anticipation and consummatory reward to food intake: a functional imaging study on healthy normal weight and overweight subjects employing intranasal insulin delivery. *Hum Brain Mapp.* **43**, 5432–5451 https://doi.org/10.1002/hbm.26019 (2022).
32. O'Doherty, J. P., Deichmann, R., Critchley, H. D. & Dolan, R. J. Neural responses during anticipation of a primary taste reward. *Neuron* **33**, 815–826 (2002).
33. Wang, G.-J. et al. Exposure to appetitive food stimuli markedly activates the human brain. *NeuroImage* **21**, 1790–1797 (2004).
34. Adamson, K. & Troiani, V. Distinct and overlapping fusiform activation to faces and food. *NeuroImage* **174**, 393–406 (2018).
35. Kroemer, N. B. et al. Fasting levels of ghrelin covary with the brain response to food pictures. *Addict. Biol.* **18**, 855–862 (2013).
36. Kroemer, N. B. et al. (Still) longing for food: insulin reactivity modulates response to food pictures. *Hum. Brain Mapp.* **34**, 2367–2380 (2013).
37. Stice, E., Burger, K. & Yokum, S. Caloric deprivation increases responsivity of attention and reward brain regions to intake, anticipated intake, and images of palatable foods. *NeuroImage* **67**, 322–330 (2013).
38. Nguyen, N. D. et al. Cortical reactivations predict future sensory responses. *Nature* **625**, 110–118 (2024).
39. Wolever, T. M., Zurbau, A., Koecher, K. & Au-Yeung, F. The effect of adding protein to a carbohydrate meal on postprandial glucose and insulin responses: a systematic review and meta-analysis of acute controlled feeding trials. *J. Nutr.* **154**, 2640–2654 (2024).
40. Forde, C. G., Mars, M. & De Graaf, K. Ultra-processing or oral processing? A role for energy density and eating rate in moderating energy intake from processed foods. *Curr. Dev. Nutr.* **4**, nzaa019 (2020).
41. Angelopoulos, T. et al. The effect of slow spaced eating on hunger and satiety in overweight and obese patients with type 2 diabetes mellitus. *BMJ Open Diabetes Res. Care* **2**, e000013 (2014).
42. Bunn, A. et al. dplR: Dendrochronology program library in R. Version 1.7.8. *CRAN* https://doi.org/10.32614/CRAN.package.dplR (2007).
43. Zhang, Z., Mai, Y., Yang, M., Xu, Z. & McNamara, C. WebPower: basic and advanced statistical power analysis. R package version 0.9.4. *CRAN* https://cran.r-project.org/web/packages/WebPower/index.html (2023).
44. Baugh, M. E. et al. Validity and reliability of a new whole room indirect calorimeter to assess metabolic response to small calorie loads. *PLoS ONE* **19**, e0304030 (2024).
45. Peirce, J. et al. PsychoPy2: experiments in behavior made easy. *Behav. Res. Methods* **51**, 195–203 (2019).
46. Lim, J., Wood, A. & Green, B. G. Derivation and evaluation of a labeled hedonic scale. *Chem. Senses* **34**, 739–751 (2009).
47. Becker, G. M., Degroot, M. H. & Marschak, J. Measuring utility by a single-response sequential method. *Behav. Sci.* **9**, 226–232 (1964).
48. Smith, S. M. et al. Advances in functional and structural MR image analysis and implementation as FSL. *NeuroImage* **23**, S208–S219 (2004).
49. Andersson, J. L. R., Skare, S. & Ashburner, J. How to correct susceptibility distortions in spin-echo echo-planar images: application to diffusion tensor imaging. *NeuroImage* **20**, 870–888 (2003).
50. Desikan, R. S. et al. An automated labeling system for subdividing the human cerebral cortex on MRI scans into gyral based regions of interest. *NeuroImage* **31**, 968–980 (2006).
51. Hutelin, Z. Metabolic and neural responses to ultraprocessed foods: a randomized, controlled, crossover study. *University Libraries, Virginia Tech* https://doi.org/10.7294/32077803 (2026).

52. Hutelin, Z. Ultraprocessed foods elicit distinct metabolic and neural responses when compared to non-ultraprocessed foods. [Dataset]. *OpenNeuro* https://doi.org/10.18112/openneuro.ds007693.v1.0.0 (2026).

Acknowledgements

We thank M. Fowler and B. Carter for performing the blood draws, Brenda M. Davy for guidance throughout the study, as well as R. McMillian, H. Zhang, and C. Najt and J. Drake of the Metabolism Core at Virginia Tech for assaying the blood samples.

Author contributions

Z.H. was responsible for the conceptualization, validation, data curation, formal analysis, visualization, investigation, methodology, project administration and writing of the original draft of the manuscript. M.A. performed data curation, formal analysis, visualization and manuscript review and editing. M.E.B. was involved with conceptualization, validation, methodology and manuscript review and editing. E.N. performed formal analysis along with manuscript review and editing. D.L.H. assisted with validation, methodology and manuscript review and editing. A.L.H. was responsible for funding acquisition, supervision, formal analysis and manuscript review and editing. A.G.D. was responsible for funding acquisition, conceptualization, creating methodology, project administration, formal analysis and manuscript review and editing.

Funding

This study was supported by R01 DK132389 to A.G.D. and a National Science Foundation Graduate Research Fellowship (2235205) to Z.H. The funders had no role in study design, data collection and analysis, decision to publish or preparation of the manuscript.

Competing interests

The authors declare no competing interests.

Additional information

Extended data is available for this paper at https://doi.org/10.1038/s42255-026-01619-4.

Supplementary information The online version contains supplementary material available at https://doi.org/10.1038/s42255-026-01619-4.

Correspondence and requests for materials should be addressed to Alexandra G. DiFeliceantonio.

Peer review information *Nature Metabolism* thanks Carlos Monteiro, Marc Tittgemeyer and the other, anonymous, reviewer(s) for their contribution to the peer review of this work. Primary Handling Editor: Jean Nakhle, in collaboration with the *Nature Metabolism* team. Peer reviewer reports are available.

Reprints and permissions information is available at www.nature.com/reprints.

Publisher's note Springer Nature remains neutral with regard to jurisdictional claims in published maps and institutional affiliations.

Open Access This article is licensed under a Creative Commons Attribution-NonCommercial-NoDerivatives 4.0 International License, which permits any non-commercial use, sharing, distribution and reproduction in any medium or format, as long as you give appropriate credit to the original author(s) and the source, provide a link to the Creative Commons licence, and indicate if you modified the licensed material. You do not have permission under this licence to share adapted material derived from this article or parts of it. The images or other third party material in this article are included in the article's Creative Commons licence, unless indicated otherwise in a credit line to the material. If material is not included in the article's Creative Commons licence and your intended use is not permitted by statutory regulation or exceeds the permitted use, you will need to obtain permission directly from the copyright holder. To view a copy of this licence, visit http://creativecommons.org/licenses/by-nc-nd/4.0/.

© The Author(s) 2026

https://doi.org/10.1038/s42255-026-01619-4

Extended Data Table 1 | Participant Characteristics

Variable	Overall
n	57
Demographics	
Age (mean (SD))	26.21 (6.85)
Sex = Male (n (%))	18 (31.6)
Income in thousands (USD) (mean (SD))	133.29 (171.68)
Race	
Asian (n (%))	12 (21.1)
Black (n (%))	2 (3.5)
More than one race (n (%))	4 (7.0)
White (n (%))	39 (68.4)
Anthropometrics	
BMI (kg/m_2) (mean (SD))	22.75 (1.87)
Waist-to-Hip Ratio (mean (SD))	0.76 (0.09)
Hemoglobin A1c[a] (mean (SD))	5.1 (0.3)
Eating behavior (TFEQ)	
Cognitive restraint score (mean (SD))	8.3 (4.5)
Disinhibition score (mean (SD))	4.8 (2.6)
Perceived hunger score (mean (SD))	4.8 (3.0)
Physical activity (IPAQ Short)	
Vigorous (min/week) (mean (SD))	279.4 (293.1)
Moderate (min/week) (mean (SD))	350.1 (683.8)
Walking (min/week) (mean (SD))	441.0 (638.1)
Sitting (min/day) (mean (SD))	444.0 (176.2)
Habitual Diet[b]	
Total Energy (kcal/day) (mean (SD))	3519.1 (1017.4)
Fat (g/day) (mean (SD))	147.2 (50.8)
Carbohydrates (g/day) (mean (SD))	402.2 (122.0)
Protein (g/day) (mean (SD))	155.5 (55.0)
Added Sugar (g/day) (mean (SD))	87.6 (54.8)
Fiber (g/day) (mean (SD))	35.7 (14.4)
UPF Intake (% total energy) (mean (SD))	54.4 (18.4)
UPF Intake (% total grams) (mean (SD))	24.6 (13.7)

BMI: Body Mass Index. TFEQ: Three Factor Eating Questionnaire. IPAQ: International Physical Activity Questionnaire. UPF: Ultraprocessed Food. an = 32 participants. bn = 55 participants.

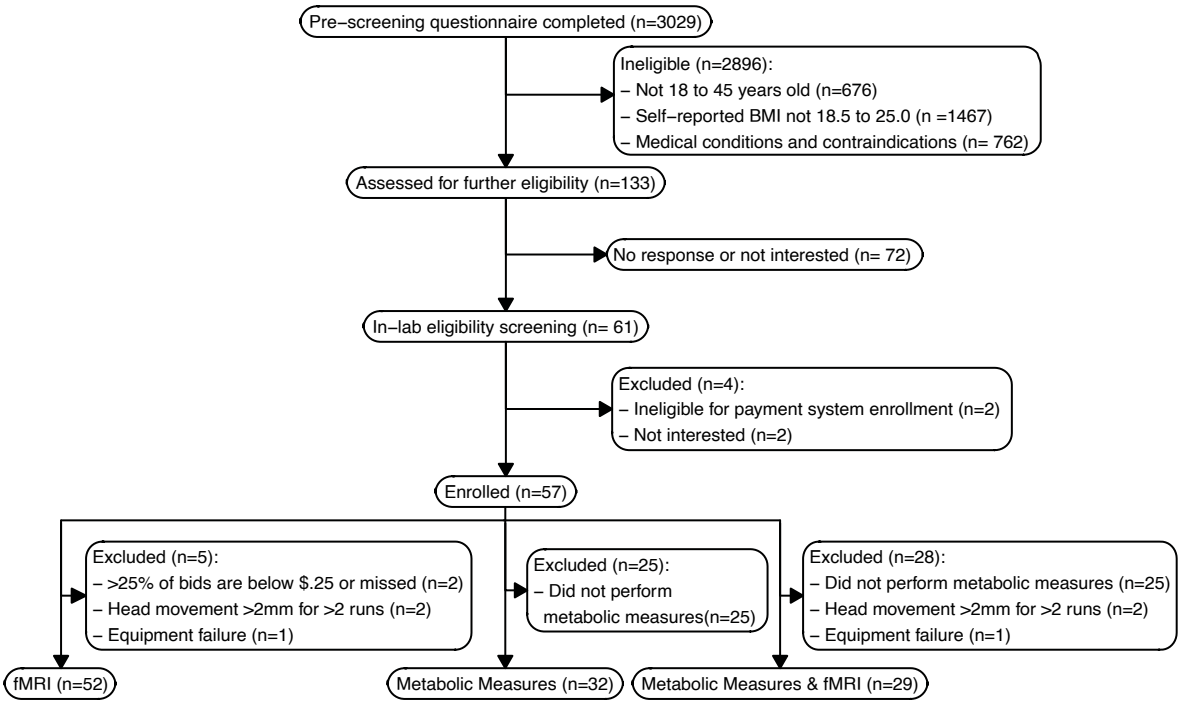
https://doi.org/10.1038/s42255-026-01619-4

Extended Data Table 2 | fMRI results from all analyses

Food Cue Reactivity Model - Peak Carbohydrate Oxidation (non-UPF - UPF), n=29						
Whole Brain Analysis	**Region**	**p(FWE-corr)**	**t**	**x [mm]**	**y [mm]**	**z [mm]**
non-UPF > UPF	L Superior Temporal Gyrus	0.013	7.33	−44	−24	−8
Region of Interest Analysis	Region	p(SVC-corr)	t	x [mm]	y [mm]	z [mm]
non-UPF > UPF	R Caudate	0.007	6.11	6	10	4
	L Ventral Striatum	0.045	5.20	−8	6	−10
Food Cue Reactivity Model - Peak Respiratory Exchange Ratio (non-UPF - UPF), n=29						
Whole Brain Analysis	Region	p(FWE-corr)	t	x [mm]	y [mm]	z [mm]
non-UPF > UPF	L Superior Temporal Gyrus	0.007	7.63	−44	−24	−8
Region of Interest Analysis	Region	p(SVC-corr)	t	x [mm]	y [mm]	z [mm]
non-UPF > UPF	R Caudate	0.014	5.77	4	8	2
	R Caudate	0.026	5.48	22	−12	24
Willngness to Pay Parametric Modulation Model, n=52						
Whole Brain Analysis	Region	p(FWE-corr)	t	x [mm]	y [mm]	z [mm]
Positive	L Orbitofrontal Cortex	0.001	6.27	−28	24	−34
	L Orbitofrontal Cortex	0.005	5.78	−24	30	−20
	R Cerebellum	0.002	6.00	42	−60	−40
	R Fusiform Gyrus	0.008	5.64	46	−62	−14
	R Lateral Occipital Cortex	0.014	5.50	44	−78	−6
	R Bed Nucleus of the Stria Terminalis	0.006	5.71	−10	2	−4
	L Intraparietal Sulcus	0.019	5.43	−28	−68	44
	L Intraparietal Sulcus	0.046	5.18	−26	−60	38
	L Posterior Cingulate Cortex	0.020	5.41	−4	−30	34
	L Pregenual Anterior Cingulate Cortex	0.021	5.40	−14	52	4
	L Pregenual Anterior Cingulate Cortex	0.043	5.20	−6	52	2
	L Temporal Lobe	0.031	5.30	−58	−42	−12
	L Putamen/Amygdala border	0.040	5.22	−32	10	−12
Negative	L Secondary Visual Cortex	0.042	5.21	−10	−64	−4
non-UPF > UPF	L Fusiform Gyrus	<0.0001	7.89	−32	−52	−14
	L Lingual Gyrus	<0.0001	7.32	−22	−84	−14
	L Lingual Gyrus	0.0001	6.69	−24	−74	−8
Region of Interest Analysis	Region	p(SVC-corr)	t	x [mm]	y [mm]	z [mm]
non-UPF > UPF	R Putamen	0.017	4.62	32	−4	12
	R Caudate	0.043	4.34	14	16	4

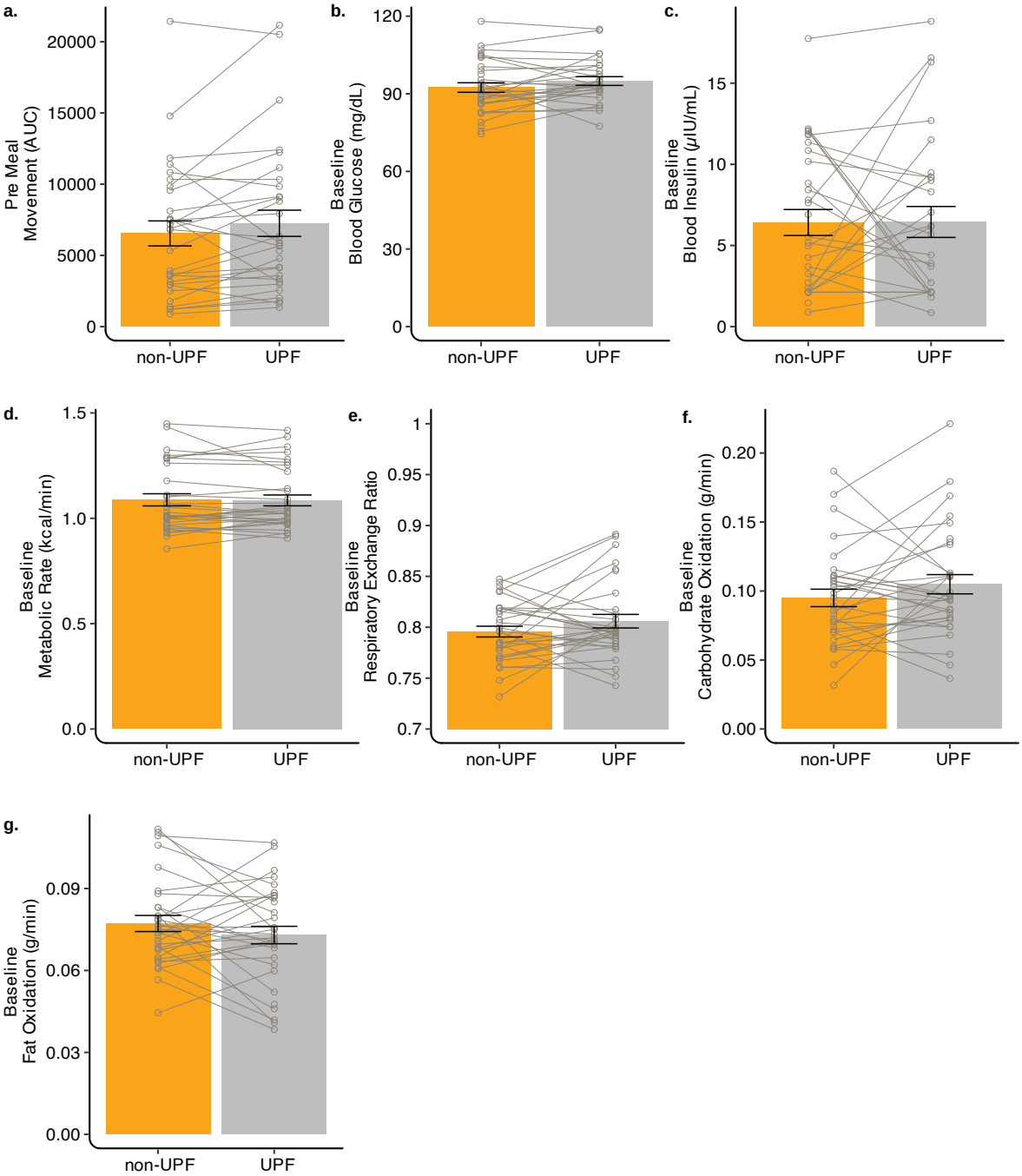
FWE: familywise error correction, SVC: small volume correction with familywise error correction, UPF: ultraprocessed food, non-UPF: non-ultraprocessed food.

https://doi.org/10.1038/s42255-026-01619-4



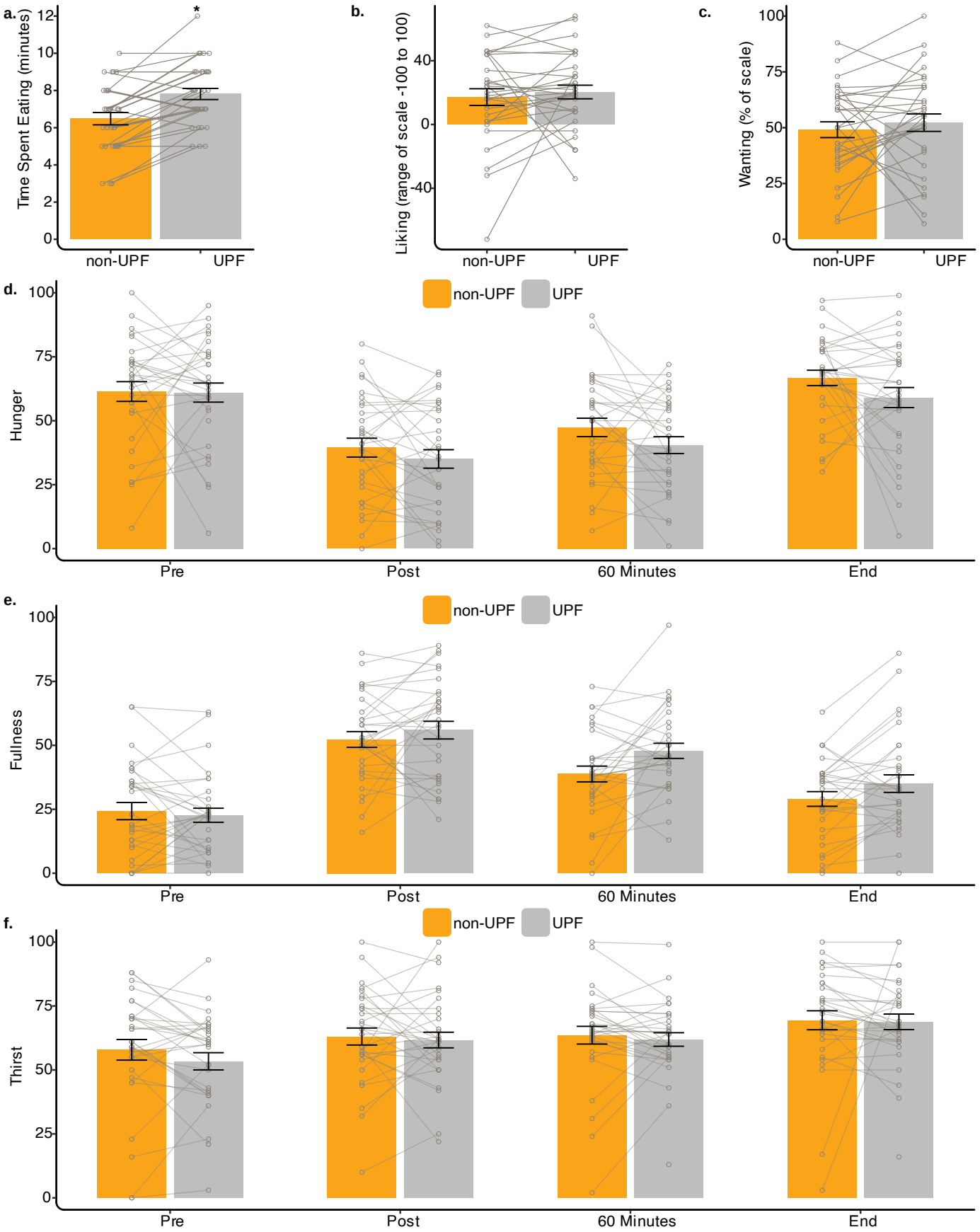
Extended Data Fig. 1 | CONSORT diagram. A general participant screening survey is used for the lab, resulting in a high number of pre-screens. After assessing eligibility, 133 participants were contacted and 61 scheduled for in-person screening. Participants were included in multiple analyses, and reasons for exclusion are noted for each analysis type. Final samples for each analysis type are in the bottom row. BMI: body mass index.

https://doi.org/10.1038/s42255-026-01619-4



Extended Data Fig. 2 | Baseline measurements from the metabolic chamber session. There were no differences across conditions among all baseline measures assessed: **a**) pre meal movement as measured by accelerometers. t(28.46) = 1.73, p = 0.10, 95% CI [−1771.61, 150.57]) **b**.) blood glucose (mg/dL) (t(26.46) = 1.43, p = 0.17, 95% CI [−5.11, 0.93]) **c**.) blood insulin (μIU/mL) (t(28.91) = 0.04, p = 0.97, 95% CI [−2.27, 2.09]) **d**.) metabolic rate (kcal/min) (t(30.10) = 0.06, p = 0.95, 95% CI [−0.02, 0.02]) **e**.) respiratory exchange ratio (t(29.99) = 1.41, p = 0.17, 95% CI [−0.024, 0.004]) **f**.) carbohydrate oxidation (g/min) (t(30.49) = 1.40, p = 0.17, 95% CI [−0.023, 0.004])**g**.) fat oxidation g/min (t(29.95) = −1.22, p = 0.23, 95% CI [−0.003, 0.01]). Each dot represents a participant and error bars represent standard error of the mean. (n = 32 participants for all analysis except blood insulin which is n = 31 participants). All tests are two-tailed.

https://doi.org/10.1038/s42255-026-01619-4

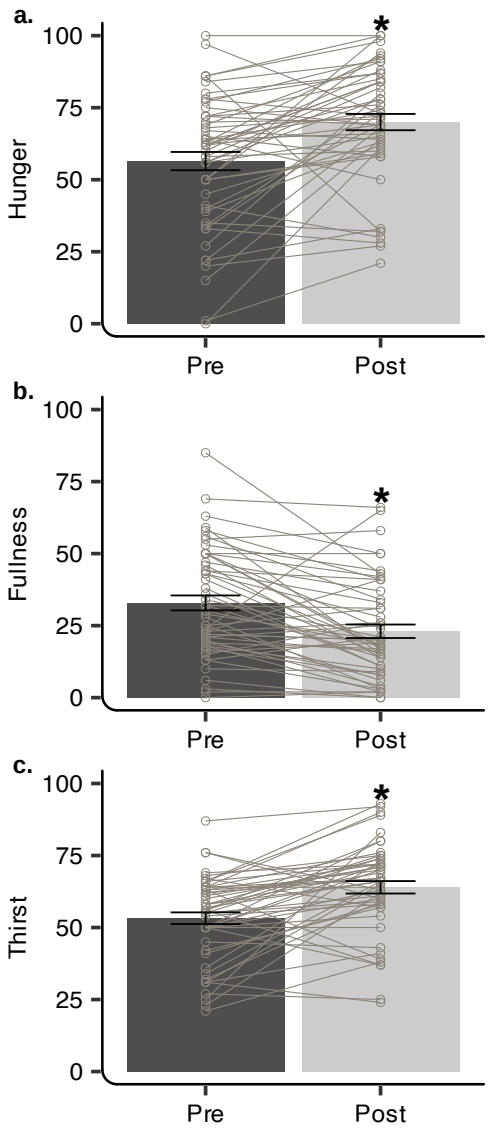


Extended Data Fig. 3 | See next page for caption.

https://doi.org/10.1038/s42255-026-01619-4

Extended Data Fig. 3 | Eating rate and food ratings during metabolic sessions. a.) The ultraprocessed meal was consumed more slowly than the non-ultraprocessed meal ($t(30.43) = 5.13$, $p < 0.001$, 95% CI [−1.82, −0.78]). All other measures including **b**.) liking ($t(30.13) = 0.61$, $p = 0.55$, 95% CI [−15.07, 8.12]) **c**.) wanting ($t(30.87) = 0.73$, $p = 0.47$, 95% CI [−12.41, 5.88]) **d**.) hunger ($\chi^2(3) = 2.05$, $p = 0.56$), **e**.) fullness ($\chi^2(3) = 6.19$, $p = 0.10$), **f**.) thirst ($\chi^2(3) = 0.76$, $p = 0.86$) did not have a significantly time by condition interaction. Each dot represents a participant, and error bars represent standard error of the mean. (n = 32 participants) *$p < 0.05$ and all tests are two-tailed.

https://doi.org/10.1038/s42255-026-01619-4



Extended Data Fig. 4 | Pre- and post-scan ratings of internal state. **a**.) Hunger was moderate and increased across the fMRI session ($t(51) = 4.69$, $p < 0.001$, 95% CI [−19.34, −7.74]), **b**.) fullness decreased over the course of the session ($t(51) = 4.98$, $p < 0.001$, 95% CI [−15.06, −6.4]), and **c**.) thirst increased ($t(51) = -4.70$, $p < 0.001$, 95% CI [5.64, 14.05]). Each dot represents a participant, and error bars represent standard error of the mean. (n = 52 participants) *$p < 0.05$ and all tests are two-tailed.

nature portfolio

Corresponding author(s): Alexandra Gold DiFeliceantonio

Last updated by author(s): Aug 17, 2026

Reporting Summary

Nature Portfolio wishes to improve the reproducibility of the work that we publish. This form provides structure for consistency and transparency in reporting. For further information on Nature Portfolio policies, see our Editorial Policies and the Editorial Policy Checklist.

Statistics

For all statistical analyses, confirm that the following items are present in the figure legend, table legend, main text, or Methods section.

n/a	Confirmed	
☐	☒	The exact sample size (*n*) for each experimental group/condition, given as a discrete number and unit of measurement
☐	☒	A statement on whether measurements were taken from distinct samples or whether the same sample was measured repeatedly
☐	☒	The statistical test(s) used AND whether they are one- or two-sided *Only common tests should be described solely by name; describe more complex techniques in the Methods section.*
☐	☒	A description of all covariates tested
☐	☒	A description of any assumptions or corrections, such as tests of normality and adjustment for multiple comparisons
☐	☒	A full description of the statistical parameters including central tendency (e.g. means) or other basic estimates (e.g. regression coefficient) AND variation (e.g. standard deviation) or associated estimates of uncertainty (e.g. confidence intervals)
☐	☒	For null hypothesis testing, the test statistic (e.g. *F*, *t*, *r*) with confidence intervals, effect sizes, degrees of freedom and *P* value noted *Give P values as exact values whenever suitable.*
☒	☐	For Bayesian analysis, information on the choice of priors and Markov chain Monte Carlo settings
☐	☒	For hierarchical and complex designs, identification of the appropriate level for tests and full reporting of outcomes
☒	☐	Estimates of effect sizes (e.g. Cohen's *d*, Pearson's *r*), indicating how they were calculated

Our web collection on statistics for biologists contains articles on many of the points above.

Software and code

Policy information about availability of computer code

Data collection	Participants completed questionnaires using REDCap electronic data capture tools. Food ratings including the fMRI task were made with PsychoPy3 (v2023.1.0). Body weight was measured with an electronic scale (Health O Meter ProPlus digital scale) and height was measured with a wall-mounted stadiometer. Waist and hip circumference were measured using Gulick tape measure following World Health Organization protocols (Waist Circumference and Waist-Hip Ratio, n.d.) for the calculation of waist-to-hip ratio. Dietary recalls were performed using the multi pass method and recorded into Nutrition Data System for Research (NDSR; version 2022; University of Minnesota, Minneapolis, MN). A small-volume whole room indirect calorimeter (WRIC) (MEI Research, Ltd) was used to measure participants' metabolic rate, respiratory exchange ratio, carbohydrate oxidation, and fat oxidation (Baugh et al., 2024). For blood sample analyses, glucose concentrations were measured in duplicate using a point of care system (Hemocue Glucose 201 System, HemoCue, CA, USA), insulin concentrations were quantified using an enzyme-linked immunosorbent assay (ELISA; ALPCO, NH, USA), and Hemoglobin A1c was determined with a point of care analyzer (Afinion HbA1c, Abbott Laboratories, IL, USA). Throughout the metabolic session participants were also fitted with accelerometers (ActiGraph wGT3X-BT) on their right wrist and left ankle to measure movement (LaMunion et al., 2017). All MRI data were acquired with a 3 Tesla Siemens MAGNETOM Prisma scanner using a 64-channel head coil. Data and code underlying this manuscript are available from the Virginia Tech Data Repository at https://doi.org/10.7294/32077803.
Data analysis	All statistical analyses on metabolic and behavioral data were conducted with R version 4.4.1 (2024-06-14). fMRI data were preprocessed and analyzed with FSL version 6.0.7.17 (FMRIB Software Library) and SPM Version 25.01.02 (Statistical Parametric Mapping) implemented in MATLAB R2021b. Data and code underlying this manuscript are available from the Virginia Tech Data Repository at https://doi.org/10.7294/32077803.

For manuscripts utilizing custom algorithms or software that are central to the research but not yet described in published literature, software must be made available to editors and reviewers. We strongly encourage code deposition in a community repository (e.g. GitHub). See the Nature Portfolio guidelines for submitting code & software for further information.

Data

Policy information about availability of data

All manuscripts must include a data availability statement. This statement should provide the following information, where applicable:

- Accession codes, unique identifiers, or web links for publicly available datasets
- A description of any restrictions on data availability
- For clinical datasets or third party data, please ensure that the statement adheres to our policy

Data underlying this manuscript are available from the Virginia Tech Data Repository at https://doi.org/10.7294/32077803. Neuroimaging data have been deposited on OpenNeuro, accession number ds007693.

Research involving human participants, their data, or biological material

Policy information about studies with human participants or human data. See also policy information about sex, gender (identity/presentation), and sexual orientation and race, ethnicity and racism.

Reporting on sex and gender	Sex was considered in the study design. Participants self-reported their sex in response to the question, "What sex were you assigned at birth?" Gender identity was also assessed using the question, "What best describes your gender identity?"; however, gender was not included in the present analyses. The final sample consisted of 18 males and 39 females, as reported in Table 1 and the Results section. Sex was included as a covariate in all fMRI models. Additionally, sex was entered as a covariate in the willingness-to-pay analyses, and the results were unchanged.
Reporting on race, ethnicity, or other socially relevant groupings	Participants self-reported their race in response to the question, "Please select the race(s) which best describe you." The following response options were provided: White; Black or African American; American Indian or Alaska Native; Asian Indian; Chinese; Filipino; Japanese; Korean; Vietnamese; Other Asian; Native Hawaiian or Other Pacific Islander; Guamanian or Chamorro; Samoan; Other; and Prefer not to disclose. Race is reported in Table 1 but was not included in subsequent analyses.
Population characteristics	See below.
Recruitment	Study participants were recruited from the University and surrounding community in Roanoke, Virginia through social media advertisements, campus advertisements, and flyers. Interested individuals filled out a general online screening form on Ripple Science software from June 2023 to December 2025 to provide self-report information for the determination of study eligibility.
Ethics oversight	All study protocols were given ethical approved by the Virginia Tech IRB (#21-1052).

Note that full information on the approval of the study protocol must also be provided in the manuscript.

Field-specific reporting

Please select the one below that is the best fit for your research. If you are not sure, read the appropriate sections before making your selection.

☐ Life sciences ☒ Behavioural & social sciences ☐ Ecological, evolutionary & environmental sciences

For a reference copy of the document with all sections, see nature.com/documents/nr-reporting-summary-flat.pdf

Behavioural & social sciences study design

All studies must disclose on these points even when the disclosure is negative.

Study description	The study used a randomized, within-participant crossover design in which quantitative data were collected.
Research sample	Study participants were recruited from the University and surrounding community in Roanoke, Virginia through social media advertisements, campus advertisements, and flyers. Interested individuals filled out a general online screening form on Ripple Science software from June 2023 to December 2025 to provide self-report information for the determination of study eligibility. To be eligible individuals had to be age 18 to 45 with a BMI between 18.5 and 25 (calculated from reported height and weight). Exclusion criteria included having dietary restrictions (food allergies, vegetarian, keto, etc.), medical conditions (including metabolic, neurologic, or psychiatric disorders) or medications used to treat these disorders, currently pregnant, current inhaled nicotine use, other recreational drugs other than periodic cannabis use, impaired taste or smell, contraindications for MRI, and vision not correctable to see MRI screen. Eligible individuals were invited for in person screening and consent.
Sampling strategy	Power analysis (Behavior). The overall sample size was estimated based on behavioral data from 11. Sample size was calculated in R 48 based on a repeated measures ANOVA model, and detecting differences in willingness to pay (bid amount in USD) among the degree of food processing condition groups 49. With a total sample size of 52 participants, pairwise comparisons among the two groups yielded 80% power to detect an effect size of Cohen's f=0.40 with a type I error rate of 5%. Based on this total sample size of 52, power was estimated for a generalized linear mixed-effects model, regressing the primary outcome (willingness to pay) on food

processing, sex, their two-way interaction, and controlling for potential confounders (hunger, energy expenditure, blood glucose, blood insulin). This was accomplished using 5,000 iterations of a Monte Carlo simulation, expected assumptions were based on the bidding data published in DiFeliceantonio et al. 11. In these simulations, the model parameters were estimated via restricted maximum likelihood, such that the specified model was compared to the null model using the likelihood ratio test, yielding 99% power to detect a statistically significant test at the 5% level of significance. In summary, a sample size of 52 participants provides sufficient power to detect a main effect difference in willingness to pay by food processing group. Power analysis (Associations between metabolism and fMRI). An ad hoc power analysis was conducted to ensure power was achieved for the subset of participants in the correlations between metabolic with brain responses. In the literature, the most relevant data are from Veldhuizen et al 2017, who reported a correlation of r=.83, which is much larger than the effect sizes used to power the study 15. We performed a power analysis based on a test of Pearson's correlation with that value. To achieve 95% power, 16 participants were needed at a significance level of .0001. Power analysis (Metabolism). A separate power analysis was conducted to evaluate the sample size needed to detect a difference in metabolic response to the meals consumed in the whole room indirect calorimeter. There was over 80% power to detect a difference, based on a paired t-test, in the AUC for energy expenditure, assuming a Cohen's d of .57 (medium size) and sample size of 27. Data collection and analysis were not performed blind to the conditions of the experiment

Data collection

All participant data were collected using a computer-based interface. No individuals were present during data collection other than the participant and the researcher, except for the MRI operator during the collection of neuroimaging data and the phlebotomist during intravenous blood draws. The researcher was involved in study design and therefore was not blinded to the study hypotheses. Additionally, blinding to experimental condition was not feasible, as the conditions consisted of distinct food items, but participants were not explicitly told what condition they were receiving.

Timing

Data collection started in end of June of 2023 and ended in December of 2025, and the metabolic sessions spanned end of June 2023 to March 2025.

Data exclusions

Of the 57 enrolled participants, 32 completed the metabolic sessions. All participants completed both the non-UPF and UPF conditions; however, one participant experienced a vasovagal response after the 60-min blood draw, resulting in early termination of that session. Due to IV patency issues, glucose samples could not be obtained for one condition in five participants. Insulin samples could not be obtained for one condition in three participants, and for both conditions in one participant. All 32 participants who completed the chamber sessions also underwent MRI scanning: two were excluded due to excessive head motion (>2 mm in ≥2 of the four runs), and one due to equipment failure.

Non-participation

A total of 61 participants completed in-lab eligibility screening. Four participants were excluded prior to enrollment (two were ineligible for the study payment system and two were not interested).

Randomization

The condition order for the metabolic sessions was randomized. The stimulus presentation order during the fMRI task was randomized using a genetic algorithm to optimize design efficiency (Wager & Nichols, 2003).

Reporting for specific materials, systems and methods

We require information from authors about some types of materials, experimental systems and methods used in many studies. Here, indicate whether each material, system or method listed is relevant to your study. If you are not sure if a list item applies to your research, read the appropriate section before selecting a response.

Materials & experimental systems

n/a	Involved in the study
☒	☐ Antibodies
☒	☐ Eukaryotic cell lines
☒	☐ Palaeontology and archaeology
☒	☐ Animals and other organisms
☐	☒ Clinical data
☒	☐ Dual use research of concern
☒	☐ Plants

Methods

n/a	Involved in the study
☒	☐ ChIP-seq
☒	☐ Flow cytometry
☐	☒ MRI-based neuroimaging

Clinical data

Policy information about clinical studies

All manuscripts should comply with the ICMJE guidelines for publication of clinical research and a completed CONSORT checklist must be included with all submissions.

Clinical trial registration

The study was registered at clinicaltrials.gov (NCT06017986).

Study protocol

The study protocol is available through the Virginia Tech Data Repository 10.7294/32077803.

Data collection

General study overview. Eligible individuals were invited for in person screening and consent. Data collection started in June of 2023 and ended in December of 2025, and the metabolic sessions spanned June 2023 to March 2025. Participants were compensated for their time.
Metabolic session. Participants completed two separate metabolic sessions on different days in a randomized crossover design. To reduce participant burden, we did not require a specific session spacing. Seven participants had sessions within 3 days, 14

participants between 4 days and 2 weeks, 7 participants between 15 days and four weeks, and finally 4 participants had sessions with a greater than 4-week gap. For each session, participants were instructed to arrive after an overnight fast and to refrain from strenuous exercise on the preceding day. Sessions were scheduled to begin in the morning, after participants' habitual wake-up time. A small-volume whole room indirect calorimeter (WRIC) (MEI Research, Ltd) was used to measure participants' metabolic rate, respiratory exchange ratio, carbohydrate oxidation, and fat oxidation for 4 hours(Baugh et al., 2024).
fMRI session. Participants were instructed to arrive neither hungry nor full, 3-hours fasted, and to refrain from strenuous exercise the day before. In relation to the metabolic sessions, 6 participants completed the fMRI session as the last session, 7 in-between metabolic sessions, and 16 as their before metabolic sessions. During this session, participants completed 4 runs of a Becker-deGroot-Marschak auction task to assess food value(Becker et al., 1964) while undergoing fMRI scanning(Newton-Fenner et al., 2023). Additional details can be found in supplemental materials.

Outcomes

This study is considered BESH (Basic Experimental Studies in Humans). Therefore, we used literature searches and expert consensus to design the experiments and identify outcomes.

Plants

Seed stocks

Report on the source of all seed stocks or other plant material used. If applicable, state the seed stock centre and catalogue number. If plant specimens were collected from the field, describe the collection location, date and sampling procedures.

Novel plant genotypes

Describe the methods by which all novel plant genotypes were produced. This includes those generated by transgenic approaches, gene editing, chemical/radiation-based mutagenesis and hybridization. For transgenic lines, describe the transformation method, the number of independent lines analyzed and the generation upon which experiments were performed. For gene-edited lines, describe the editor used, the endogenous sequence targeted for editing, the targeting guide RNA sequence (if applicable) and how the editor was applied.

Authentication

Describe any authentication procedures for each seed stock used or novel genotype generated. Describe any experiments used to assess the effect of a mutation and, where applicable, how potential secondary effects (e.g. second site T-DNA insertions, mosiacism, off-target gene editing) were examined.

Magnetic resonance imaging

Experimental design

Design type

Task, event-related design

Design specifications

Each subject completed 4 auction task trails. Each trial lasted approximately 8.5 minutes and consisted of a jittered inter trial interval (mean 4-sec) followed by a food picture presentation period (5-sec), jittered fixation point (mean 4-sec), bid rating (5-sec maximum). Trial order, inter stimulus interval, and intertrial interval were chosen using a genetic algorithm approach to optimize fMRI design (Wager & Nichols, 2003). During each trail, participants bid their willingness to pay between 0 and 5 USD on 28 different foods presented in a randomized order.

Behavioral performance measures

Bid amount ($0-$5) was collected. If more than 25% of bids were either less than $0.25 or missing across all runs, that participant was excluded.

Acquisition

Imaging type(s)

Echo Planar Images (EPI) and Magnetization-Prepared Rapid Gradient Echo (MPRAGE)

Field strength

3 Tesla

Sequence & imaging parameters

All MRI data were acquired with a 3 Tesla Siemens MAGNETOM Prisma scanner using a 64-channel head coil. Acquisition parameters for the functional echo-planar images (EPIs) were TE=34ms, echo spacing=0.66ms, TR=1.5s, flip angle=70, voxel size=2x2x2 mm, number of slices=72, and multiband acceleration factor=4. To allow distortion correction, sets of identical images were acquired with reverse (posterior-to-anterior and anterior-to-posterior) phase encoding polarity. A high quality T1 weighted anatomical image (TE=2.32ms, TR=2.3s, flip angle=8, slices=192, field of view=240mm, voxel size= 0.9x0.9x0.9 mm) was acquired for registration of functional images.

Area of acquisition

Whole brain coverage

Diffusion MRI ☐ Used ☒ Not used

Preprocessing

Preprocessing software

fMRI data were preprocessed with FSL version 6.0.7.17 (FMRIB Software Library) and SPM Version 25.01.02 (Statistical Parametric Mapping) implemented in MATLAB R2021b. Susceptibility-induced distortions were estimated using opposite phase encoded images and corrected with a Jacobian transformation using FSL (Smith et al., 2004) topup (Andersson et al., 2003). Preprocessing was then completed with SPM and includes realignment, coregistration of the functional images to each participant's T1-weighted anatomical image, and spatial smoothing with a 6mm full width half maximum gaussian kernel.

Normalization

During segmentation, nonlinear deformation fields were estimated to align each participant's anatomical T1-weighted image

Normalization	to standard space in SPM25. The resulting deformation fields were then applied to the EPI runs to warp the functional data into the standard space.
Normalization template	Group standard space, MNI-152
Noise and artifact removal	The following nuisance regressors were used for first level modeling: Friston's 24 head motion parameters (Friston et al., 1996) (6 SPM realignment parameters, 6 of their preceding values, and 12 corresponding squared terms), the mean signal extracted from the cerebrospinal fluid and white matter (along with their preceding values, and corresponding squared terms), DVARS (D referring to the temporal derivative, VARS referring to RMS variance over voxels)(Power et al., 2012; Smyser et al., 2011), and Framewise Displacement (FD) computed with fsl_motion_outliers, and a matrix of motion-outlier volumes (DVARS threshold at 75th percentile plus 1.5 times the interquartile range and/or greater than .5 mm of Framewise Displacement).
Volume censoring	Motion outlier volumes were identified as those exceeding a DVARS threshold defined as the 75th percentile plus 1.5 times the interquartile range and/or exhibiting Framewise Displacement greater than 0.5 mm. These volumes were deweighted, no volumes were removed.

Statistical modeling & inference

Model type and settings	Two first-level general linear models (GLMs) were specified. For both GLMs, the interval from the onset of the post-picture fixation period through bid submission (i.e., the participant-specific reaction time during each bidding period) was modeled as a regressor of no interest. Additional nuisance regressors as described above were entered. The first GLM was designed to capture food-cue reactivity by modeling the 5-s picture-viewing period with a boxcar regressor, with separate regressors for non-UPF and UPF trials (DiFeliceantonio et al., 2018; Tang et al., 2014). For the first GLM the non-UPF >UPF contrast was brought to the group level and used to test the association with the between-condition difference in peak metabolic response to the test meals (non-UPF – UPF) measured during the metabolic sessions using a one-sample t-test with age, sex, and metabolic difference. The second GLM was designed to capture value-related responses while accounting for measures that differed across conditions (frequency of consumption and perceived healthiness), such that effects attributed to food type were not confounded by these factors. Accordingly, the second was identical to the first but additionally included trial-wise willingness-to-pay, frequency of consumption, and perceived healthiness as parametric modulators of the 5-s picture-viewing regressor. Parametrically modulated UPF and non-UPF picture viewing was brought up to the second level in a full factorial model and the contrasts UPF>non-UPF and non-UPF>UPF were tested with sex and age as covariates.
Effect(s) tested	UPF>non-UPF, non-UPF>UPF. UPF>non-UPF metabolic response regressed against UPF>non-UPF picture viewing

Specify type of analysis: ☐ Whole brain ☐ ROI-based ☒ Both

Anatomical location(s)	Prior work has shown that peak metabolic responses are associated with striatal activation (de Araujo et al., 2013; Veldhuizen et al., 2017), and recent meta-analyses have also associated the striatum with differences in willingness to pay (Newton-Fenner et al., 2023; Y. Wang & Yao, 2024). Accordingly, we examined both GLMs using whole-brain corrected analyses and small-volume correction within an a priori striatal mask (caudate, putamen, and nucleus accumbens) derived from Harvard–Oxford atlas (Desikan et al., 2006).
Statistic type for inference (See Eklund et al. 2016)	Voxel-wise, family wise error (FWE) corrected
Correction	Corrections for multiple comparisons were applied using a voxel-wise FWE-corrected threshold of $p < 0.05$. For visualization of clusters containing the peak voxel, statistical maps are displayed at uncorrected $p < 0.001$, $k > 10$.

Models & analysis

n/a	Involved in the study
☒	☐ Functional and/or effective connectivity
☒	☐ Graph analysis
☒	☐ Multivariate modeling or predictive analysis